

## Nanoparticle Alloy Formation by Radiolysis

*J. Grand<sup>1</sup>, S.R. Ferreira<sup>2</sup>, V. de Waele<sup>3</sup>, S. Mintova<sup>1</sup> and T.M. Nenoff<sup>2\*</sup>*

<sup>1</sup>Normandie Université, ENSICAEN, UNICAEN, CNRS, Laboratoire Catalyse et Spectrochimie, 14000 Caen, France

<sup>2</sup>Sandia National Laboratories, PO Box 5800, MS-1415, Albuquerque, NM 87185 (USA)

<sup>3</sup> Univ. Lille, CNRS, UMR 8516, LASIR, Laboratoire de Spectrochimie Infrarouge et Raman, Lille, France

\*Corresponding author's E-mail: [tmnenof@sandia.gov](mailto:tmnenof@sandia.gov)

## **Abstract**

This review focuses on the highly versatile and effective method of radiolysis for the synthesis of nanoparticles (NPs). In particular, the formation of bimetallic and alloyed nanoparticles (or nanoalloys), including both known super alloys and novel alloy NPs compositions is described. This review discloses the synthesis techniques that rely on ionizing radiation sources to create metallic NPs. Then alloy NPs formed from combinations of transition metals and noble metals with varied structures are described. Some of the advantages of radiolysis including exquisite control over the size, monodispersity, and alloying structure of NPs are discussed. Additionally, methodologies that facilitate the synthesis or deposition of NPs onto a range of supports under inert environments are described. Finally, applications of metallic NPs formed by radiolysis are summarized.

## 1. Introduction

Metal nanoparticle (NP) research has continued to grow for over two decades bringing great promise with the numerous current and potential applications in fields ranging across the spectrum, including catalysis, medicine and energy.<sup>1-3</sup> With the drive for novel NP applications, focus is being placed not only on understanding the properties of metallic NPs through characterization, but also on expanding synthesis methods. This is critical to the goal of designing more novel metallic NPs with better control over structure.

A way to improve metal NP is to combine metals having complementary properties of interest, supposing that properties will combine as well. This idea led to alloys: mixtures of metal atoms having defined metallic bondings.<sup>4</sup> For example, the combination of magnetic properties of Fe NPs with plasmonic properties of Au ones has been shown by Amendola et al.<sup>5</sup> Alloys metal NPs have gain interest due to their remarkable performances towards usual metallic NP applications such as catalysis. Indeed, some alloys were found more efficient or at least behaving differently when compared to their monometallic counterparts in some catalysis applications.<sup>6-8</sup>

A variety of synthesis techniques are available for metallic NPs, and particularly alloyed, bimetallic NPs, or nanoalloys.<sup>2,9,10</sup> A recent review by Zaleska-Medynska et al. detailed metallic nanoalloys,<sup>11</sup> with overviews of the varied synthesis techniques including popular methods such as microwave heating, molecular beams, chemical reduction methods, electrochemical techniques, thermal decomposition and radiolysis. Further synthesis techniques include novel approaches such as biosynthesis and ultrasound.<sup>12,13</sup> Together, the suite of techniques available for alloyed NP synthesis provides a powerful toolbox for designing the compositions of NPs. Complementary information on the formation of metal and nanoalloy NPs can be found in these recent reviews or books.<sup>3,14,15</sup> Many of the available techniques have significant limitations in terms of the variety of applicable materials, the structures that can be formed, or in scalability. Thermal decomposition is one technique to form alloys. However, it is primarily limited to low-valent, mainly noble, metals. In chemical reduction, bimetallic particles generally form core-shell structures with

the higher redox potential metal reducing first to form the core, and the metal with the lower redox potential making up a shell. With the use of ionizing radiation, the bombardment of ions with high energy can induce structures not strictly dictated by e.g. the redox potential of elements. Molecular beams are useful for creating and studying clusters, though they are not practical for large-scale synthesis. By comparison, gamma( $\gamma$ )-radiation is an effective technique for the controlled, scalable synthesis of a wide range of transition metal alloy nanoparticles. It is also a technique that allows for the control of NP structures through variable reaction dose rates. Recent publications showed that the shape morphology of metal NP is one of the key features for their properties;<sup>16,17</sup> and can be controlled by radiolysis.<sup>18</sup>

Herein, the scope of the review paper will be to focus on the use of radiolysis for the formation of nanoalloys and NPs, and describe synthesis techniques using radiolytic chemistry. Radiolytic chemistry involves the dissociation of molecules via ionizing radiation to generate reactive chemical species. Radiolysis can be used to form a wide range of monometallic and multimetallic species from not only noble metals, but also transition metals and group 3-5 metals. Furthermore, radiolysis provides the unique capability to explore novel materials that have not been previously identified. These novel materials can be described as “kinetically driven,” meaning that the alloys or crystal structures created are not thermodynamically favored, and therefore not formed during other, lower energy synthesis techniques. Control over the dose and dose rate in radiolysis enables precise control over the formed particle characteristics, including size, shape and crystal structure. NP species and/or nanoalloys that have been synthesized by radiolysis and provide an outlook on future possible areas of discovery will be outlined, followed by a word on superalloys then, the ability to synthesize and deposited NP on a variety of supports at room temperature make radiolysis relevant to future research in nanoalloys.<sup>19</sup> Added benefits of utilizing radiolysis for the formation of NPs, in addition to the control over the size and alloying structure is the ability to form disperse nanoalloy NPs on a range of supports under inert environments. This supported synthesis offers improved distribution of the NPs, which limits their unwanted aggregation. Recent developments of this synthesis

technique will be developed below. The last synthesis technique discussion of this review will focus on the recent developments of sintering technique.

The advantage of radiolysis in the design of specially engineered nanoalloy NPs make it an exciting tool for NP synthesis research, provided that obtained NPs are fully apprehended using comprehensive characterization techniques. Methods and their scope of interest are summarized herein.

The study of NPs formation mechanisms during radiolysis is vital to understanding and designing optimal NP reaction conditions. Pulse radiolysis is particularly useful method for elucidating the mechanisms of reactions at very short time scales. Detailed theoretical and experimental studies by various groups worldwide have focused on both the reaction mechanisms in the radiolysis of water, and the mechanisms of NP formation.<sup>20-25</sup> Only experimental studies will be described below.

Finally, the intense and expansive research into nanoalloy synthesis via radiolysis is motivated by the growing body of current (and promising future) applications that take advantage of the unique properties of the NPs. Applications such as catalysis, hydrogen gas production, waste remediation, and superalloy materials development, are all positively benefitted from this research. It is well documented that the quantum size effects lead to NP properties unique from those in the bulk.<sup>26</sup> This review addresses a number of applications that are (or can be) positively affected by the development and use of nanoalloys formed by radiolysis.

## 2. Methods

Radiolytic chemistry involves the dissociation of molecules via ionizing radiation to generate reactive chemical species. Examples of such radiation sources include high energy, short wavelength high frequency electromagnetic radiation waves from the UV, X-ray and gamma ray spectrums or accelerated particle beams of electrons or ions. In a typical radiolytic synthesis, the ionizing radiation is applied to generate by interaction with the solvent (or a matrix) strong reducing species (solvated electron,  $e^-_{solv}$ , hydrogen atom,  $H^{\cdot}$ ) capable of reducing most of the metal cations dissolved in the solution (or matrix).

Radiolysis techniques offer several advantages for a controlled reduction of metal ions: (1) no addition or no use of excess of reducing agent or undesired oxidation products from the chemical reductant, (2) a well-known rate of reaction, since the number of reducing equivalents generated by radiation is well defined and fully determined by the dose deposited in the sample, (3) absorption of the energy of the radiation by the solvent (or matrix) without interference from light-absorbing solutes and products, and (4) quasi-instantaneous ( $\sim 100$  ns) formation of an uniform distribution of the reducing agent in the solution.<sup>2</sup> Moreover, the radiolysis is recognized as a mild chemical method of reduction because it proceeds usually at room temperature, and because the reducing species can be generated at a very low rate in the sample. Typically with a Gamma source, the rate of formation of reducing species can be continuously tuned from the  $\mu\text{mol L}^{-1}\text{h}^{-1}$  to the  $\text{mmol L}^{-1}\text{h}^{-1}$  ranges. The choice of the ionizing radiation allows the control of the dose rate, over several orders of magnitude. Typical dose rate employed in the preparation of core-shell and alloyed NPs are given in Table 1.

**Table 1:** Nanoalloy formation by  $\gamma$ -radiation or other ionizing radiation techniques. The resulting structures formed are either core-shell (CS) or alloyed unless otherwise noted.

Bimetallic NP	Technique	Dose rate (or dose) for CS Structure	Dose rate (or dose) for Alloy Structure	Ref.
Ag-Ni	$\gamma$ -radiation		300 Rad/s	23
Ag-Pd	$e^-$ beam		7.9 MGy/h	80
Ag-Pd	$\gamma$ -radiation	6.3 kGy/h		80
Ag-Pt	$\gamma$ -radiation		Alloyed	32
Au-Ag	$\gamma$ -radiation	0.25-3.8 kGy/h	35 kGy/h	38
Au-Ag	Laser Irradiation		5-10 ( $\text{mJ/cm}^2$ )/pulse	157
Au-Pd	$e^-$ beam		7.9 MGy/h	80
Au-Pd	$\gamma$ -radiation	6.3 kGy/h		80
Au-Pd	$\gamma$ -radiation		2.2 kGy/h	81

Au-Pd	Pulse Radiolysis	50–55 Gy/pulse (heteroaggregate)		10
Au-Pt	UV		254 nm deep-UV radiation (10 W Hg lamp)	63
Au-Pt	X-ray		$>10^{14}$ photon.mm <sup>2</sup> /s	53
Au-Pt	$\gamma$ -radiation	7.9 MGy/h (Au <sub>core</sub> -Pt <sub>Shell</sub> ) 0.2 then 21 kGy (Pt <sub>core</sub> -Au <sub>Shell</sub> )		158
Au-Pt	$\gamma$ -radiation		1.75 Gy/s	28
Au-Pt	e <sup>-</sup> beam		2200 Gy/s	28
Au-Pt	Ion beam		<sup>13</sup> C <sub>6</sub> <sup>+</sup>	28
Au-Pt	e <sup>-</sup> beam		12 kGy	72
Ce-Ni	$\gamma$ -radiation		5 kGy/h (92 kGy)	159
Cu-Fe	$\gamma$ -radiation		Alloyed	32
Cu-Pd	$\gamma$ -radiation		8 kGy	43
Cu-Pt	$\gamma$ -radiation		5 kGy/h	150
Cu-Pt	e <sup>-</sup> beam		20 kGy/several s.	74,75
Ni-Pd	$\gamma$ -radiation		300 Rad/s	82
Ni-Pt	$\gamma$ -radiation		Alloyed	32
Pt-Ru	$\gamma$ -radiation		6.48e <sup>5</sup> kGy/h	103
Pt-Ru	e <sup>-</sup> beam		3 kGy/s	73

Tuning the dose rate is particularly useful in the context of metal nanoparticles synthesis, as it is well-established that the dose rate is a crucial parameter governing the complex nucleation-growth reactions.<sup>1,27</sup> As a rule of thumb, in solution, a high dose rate favors the formation numerous nucleation centers and small NPs with a narrow particle size distribution are synthesized, whereas at low dose rate, larger NPs are usually obtained. In a similar way, the dose rate governs also the formation of alloys of bimetallic compounds.

The structure of these nanoparticles results from an equilibrium between the radiolytic reduction and the electron transfer reaction. Alloys are synthesized at high dose rate, whereas core-shell bimetallic NPs are obtained at low dose rate. Furthermore, the effect of the dose on the nucleation of silver and bimetallic gold-platinum NPs is unique per radiolysis source, such as for  $\gamma$ ,  $e^-$ , and  $C_6^+$  beam.<sup>28</sup>

The irradiation sources can be classified regarding their Linear Energy Transfer (LET), which governs the radiolytic yield of formation of the reducing species and the penetration of the radiation. Electromagnetic (EM) radiation (UV, X-ray,  $\gamma$ ) and accelerated electrons beam are low-LET ionizing radiations, while ion beams are high LET radiation. For radiations of similar LET, the radiolytic yield of formation of different radiolytic species is similar, yielding, at the same dose rate, the same chemical reactivity upon irradiation. Notably,  $\gamma$ -gamma ray and 1-10 MeV electron beams have similar LET and are therefore complementary techniques to investigate the formation of NPs by using steady state ( $\gamma$ -ray) or pulse-radiolysis ( $e^-$  beam) approaches.<sup>28,29</sup>

Numerous methods are applied toward synthesis of monometallic NPs and nanoalloys. These techniques include the standard wet chemistry based on chemical reduction, thermal decomposition of transition metal complexes, and electrochemistry.<sup>30</sup> Other synthesis techniques are common including the application of energy in the electromagnetic spectrum, from optical to gamma radiation and by bombardment using a range of ions and electron beams.<sup>31-34</sup> These energy-based techniques will be discussed in this review, including UV, X-ray, and particle beam irradiations. Particular attention to  $\gamma$ -irradiation, the most prevalent technique towards NPs and nanoalloys will be paid.

## 2.1 Gamma( $\gamma$ -)ray irradiation

Gamma( $\gamma$ -)irradiation is the most widely used electromagnetic (EM) energy source in NPs formation. It is the highest frequency EM source, although there is overlap in energy between gamma and X-ray radiation sources. This paragraph focuses on ( $\gamma$ )-irradiation while the next one will be dedicated to X-ray. There are numerous reports in the literature of using both pulsed and continuous gamma irradiation for the formation of single metal,

bimetallic, and nanoalloy NPs.<sup>20,21,28,35-37</sup> Main features of this radiolysis technique are summarized in Table 2.

**Table 2:**  $\gamma$ -irradiation approach.

<b><math>\gamma</math>-irradiation features</b>
No harsh reducing agents
Aqueous environment
Room temperature, Atmospheric pressure
Control size and morphology by mild scavengers
Specific dose rates
Non thermodynamically favored NPs
Mechanism/reactivity studies using pulse irradiation
Large scale synthesis

Synthesis of Ag NPs with gamma ( $\gamma$ -) irradiation is widely reported.<sup>38,39</sup> The Ag NPs are commonly used as a model system, because they are easily prepared by a large range of techniques. Additionally,  $\gamma$ -irradiation has been used for synthesis of other metals including Cu<sup>40,41</sup> Ru, etc.<sup>42</sup>

Alloys have been formed with gamma irradiation, and this research was pioneered by Belloni et al.<sup>32,38,43</sup> and largely developed worldwide. For alloys, by varying the dose rate of  $\gamma$ -irradiation, the structural composition of a given precursor mixture will form various structural nanoparticles. At lower dose rates, bimetallic particles form a core-shell structure if the redox potentials are sufficiently different. In order to invert the core-shell structure, core-shell NPs may also be formed through a two-step reaction procedure, in which the solution contains one metal salt and is irradiated to form the core, and then another metal salt solution is added to the reaction and re-irradiated to form the shell.<sup>1</sup> With increasing dose rate, or energy, thermodynamic barriers to phase formation may be overcome, allowing for alloying of species not formed by lower energy sources or wet chemistry techniques.<sup>1</sup> This ability to finely tune the synthesis conditions and direct the final composition provides an important advance in materials synthesis capabilities.

Gamma-rays used in radiolysis are generated almost exclusively from cobalt-60 ( $^{60}\text{Co}$ ) gamma ( $\gamma$ -sources<sup>44</sup> though they are also produced by cesium-137 ( $^{137}\text{Cs}$ )).<sup>32,45</sup> The  $\gamma$ -irradiation is produced when the  $^{60}\text{Co}$  decays to excited  $^{60}\text{Ni}$  through beta decay, and subsequently releases two gamma ray photons as it drops to the ground  $^{60}\text{Ni}$  state. Because  $\gamma$ -irradiation occurs through decay, it is a very convenient radiolysis technique requiring no specialized instrumentation other than those dealing with shielding. The  $\gamma$ -irradiation source at Sandia National Laboratories is located at the Gamma Irradiation Facility (GIF) and is a  $^{60}\text{Co}$  source:  $1.345 \times 10^5$  Curie (Ci),  $\approx 300\text{K}$  rad/h (3,000 Gray/h (Gr/h)),  $\approx 1.25\text{KeV}$ . As is typical, the  $^{60}\text{Co}$  sources are housed in a water pool to isolate the radiation. Furthermore, gamma irradiation from  $^{60}\text{Co}$  is highly uniform, and therefore the dose and dose rate may easily be tuned and maintained by placing samples at given distances from the source when the source is designed as a long cylinder of the appropriate dimensions.<sup>46</sup>

Typical  $\gamma$ -irradiation experiments to form either monometallic or bimetallic NPs involve metal precursor salts that are dissolved in deionized water, to provide the metal ions for reduction. In many cases, an alcohol (such as methanol) is added to the reaction solution, to act as an OH radical scavenger. In addition, polymer additives such as poly(vinyl alcohol) (PVA) or sodium citrate may be added as a surfactant to keep the formed NPs both dispersed and spherical in shape.<sup>23</sup> These solutions are sealed in reaction vessels, and bubbled with an inert gas (e.g., argon) to remove oxygen prior to the reaction. This reaction vessel technique has also been recently reported for the preparation of uranium nanoalloys.<sup>47</sup>

Another advantage of NP synthesis by radiolysis is its scalability. X-rays and  $\gamma$ -rays and electrons have low linear energy transfer, or energy loss per unit length of the particle path. Therefore, larger volumes of material may be irradiated by these energy sources, and larger scale synthesis may be achieved.  $\gamma$ -irradiation can be used for samples with large volumes, with uniform energy delivered which varies as a function of the distance from the source.

## 2.2 X-ray irradiation

Another electromagnetic irradiation technique applied for NPs is based on the use of X-ray irradiation from a synchrotron X-ray source<sup>48,49</sup> or from a laboratory source.<sup>50,51</sup> X-ray irradiation shares the same advantages of radiolysis techniques outlined previously, however the instrumentation is more involved, and the radiation field is much smaller and more difficult to be controlled and tuned. For example, the synchrotron X-ray source used by Lee *et al.*, was a 2.5 GeV with a white beam confined to 0.5 x 0.5 cm<sup>2</sup> to form Ni nanoparticles.<sup>52</sup>

However, the use of X-ray irradiation for the formation of alloys is rare. It has been only reported once, explicitly on the formation of AuPt alloy.<sup>53</sup> Intense X-ray irradiation from a synchrotron facility (> 10<sup>14</sup> photon.mm<sup>2</sup>.s<sup>-1</sup>) has been necessary to form AuPt alloys in the presence of polyethylene glycol.

X-ray irradiation is more commonly associated with monometallic nanoparticle synthesis, mainly gold or nickel nanoparticles have been synthesized. In addition, two examples of X-ray irradiation promoting the silver NPs formation has been reported independently by Zhang *et al.*<sup>54</sup> and Remita *et al.*<sup>55</sup> Several recent reports using in situ measurements study the mechanism using tetrachloroaurate as precursors in different media.<sup>56,57</sup> The reaction, named Synchrotron X-ray induced reduction, involves the reduction of metal ions by the radicals in situ generated by the irradiation of water, inorganic salts or ionic liquids.<sup>58</sup> More recently, Yamaguchi *et al.* confirmed that synchrotron X-ray irradiation provides hydrogen and hydroxyl radicals from water which produced Au NPs by a redox reaction.<sup>59</sup> In addition, the same group demonstrated that synchrotron X-ray irradiation can also induced the formation of Fe or Cu particles.<sup>60</sup> The use of ethanol as additive was required only in the case of Cu NPs. Indeed, the authors reported that the use of ethanol enabled the nucleation and growth of Cu particles. On the contrary, no Cu particles were obtained using a copper sulfate solution without ethanol addition.

### 2.3 UV irradiation

UV-irradiation is the lowest ionizing energy electromagnetic technique, and it is also employed for preparation of NPs.<sup>61</sup> UV is used in monometallic<sup>62</sup> and alloy nanoparticle

formation.<sup>63</sup> Monometallic Pd NPs were synthesized using a 450 W Hg lamp to irradiate a PdCl<sub>2</sub> solution.<sup>64</sup> Alloy Au-Pt NPs are formed within a Poly(methyl methacrylate) matrix using a 10 W Hg lamp to produce 254 nm deep-UV radiation, which induce the alloy formation.<sup>63</sup>

## 2.4 Particle beam source irradiation

Another category of irradiation techniques comes from particle beam sources. Similar to EM radiolysis techniques, particle beams are high-energy sources for radiolysis induced nanoparticle synthesis. Particle beams are used to obtain irradiation over a range of energies. Ion beam irradiation including very high energy swift heavy ions<sup>65</sup> have been used for metallic NPs<sup>28,66-68</sup> and alloy formation.<sup>28</sup> Electron beam irradiation has also been used for metallic alloy formation.<sup>28</sup>

MeV electron-beams generated by LINAC accelerators are routinely applied for the preparation of metal nanoparticles and alloys under high dose rate delivering condition (> kGy/s)<sup>28,29,69</sup>. The e<sup>-</sup> beam facilities are the appropriate to scale the radiolytic approach at the industrial level. As an alternative for the NPs preparation, microbeam of accelerated electrons in the TEM enable spatially resolved and in situ preparation and characterization.<sup>70</sup> On the opposite side of the energy spectra, nearly-thermal electron (0.1 eV) were successfully used to prepare at high rate, surfactant free gold nanoparticles in micro-droplets.<sup>71</sup>

Concerning gold containing nanoparticles, Au-Pt alloys have also been formed using electron beam irradiation with a 20 kW and 10 MeV electron accelerator.<sup>72</sup> Using electron beam irradiation, the effect of promoters has been studied for the formation of Pt-based alloys. A chelate agent, tartaric acid, has been added to enhance alloying potential of Pt and Ru supported on a carbon support during irradiation with an electron beam of 4.8 MeV at room temperature (3 kGy/s).<sup>73</sup> More recently, the same group proposed the use of ethylene glycol as organic stabilizer to promote Pt-Cu alloys formation using the same electron beam irradiation process.<sup>74</sup> The authors claimed that the ethylene glycol protects

the Cu metallic clusters and prevent them from competing oxidation reaction. The effect of carboxylate containing compounds on platinum growth has also been studied.<sup>75</sup>

## 2.5 Pulse radiolysis

Pulse radiolysis is mostly used to study the electron-metal interactions occurring during the formation of monometallic and bimetallic nanoparticles (see below: Mechanism). Indeed, few publications described its use for the synthesis of metallic particles, and even less for alloys. The first example was reported by Treguer et al.<sup>38</sup> The authors demonstrated that pulse radiolysis of  $\text{Ag}^+$  and  $\text{AuCl}_4$  solutions afforded alloyed nanoparticles at  $7.9 \cdot 10^3$  kGy/h dose rates, while lower doses rates (35 kGy/h) gave bilayered materials. Later, pulse radiolysis has been used to form Au-Pd particles but only hetero-aggregates have been obtained.<sup>10</sup>

## 3. Results & Discussions

While the majority of radiolytic syntheses are used to form monometallic NPs, there have been efforts in many labs in using various radiolysis techniques to form alloy NPs.

### 3.1 Alloy Nanoparticles by Radiolysis

#### 3.1.1 Synthesis scope

Some of the most widely reported materials used to form NPs by radiolysis are those of the noble metals including Ag, Au and Pt. While these may readily be synthesized by numerous techniques, they are used in a number of studies to understand the synthesis and reaction mechanisms.<sup>76,77</sup> However, radiolysis is broadly applicable, and has been used in the synthesis of NPs from numerous metals. In addition to the noble metals, radiolysis has been used to form metal NPs including Co, Ni, Cu, Zn, Mo, Ru, Rh, Pd, Ag, Cd, In, Sn, Sb, Os, Ir, Pt, Au, Hg, Tl, Pb and Bi.<sup>32</sup>

Through the addition of a second metallic component, improvements in the stability and selectivity of pure metallic NPs are possible. By forming bimetallic nanoalloys it is possible to create NPs that exhibit optical, catalytic, and magnetic properties, which depend

on the structure and composition of the NPs.<sup>2</sup> Consequently, increasing research has concentrated on the synthesis of such varied nanoalloys. These NPs can be formed either as core-shell segregated nanoalloys, subcluster segregated nanoalloys, mixed order or mixed random nanoalloys, and multi-shell nanoalloys, or as core-shell nanoparticles.<sup>2,78</sup> Table 1 lists bimetallic NPs formed by  $\gamma$ -radiation,  $e^-$  beam irradiation or other methods. By varying the dose rate, the same precursors may be made into a segregated core-shell structure or an alloy, as seen with Au-Pd.<sup>79</sup> Alternatively, varying reaction conditions (precursors type, one-step or two-step processes) can also provide both types of structure (Figure 1).<sup>80,81</sup>

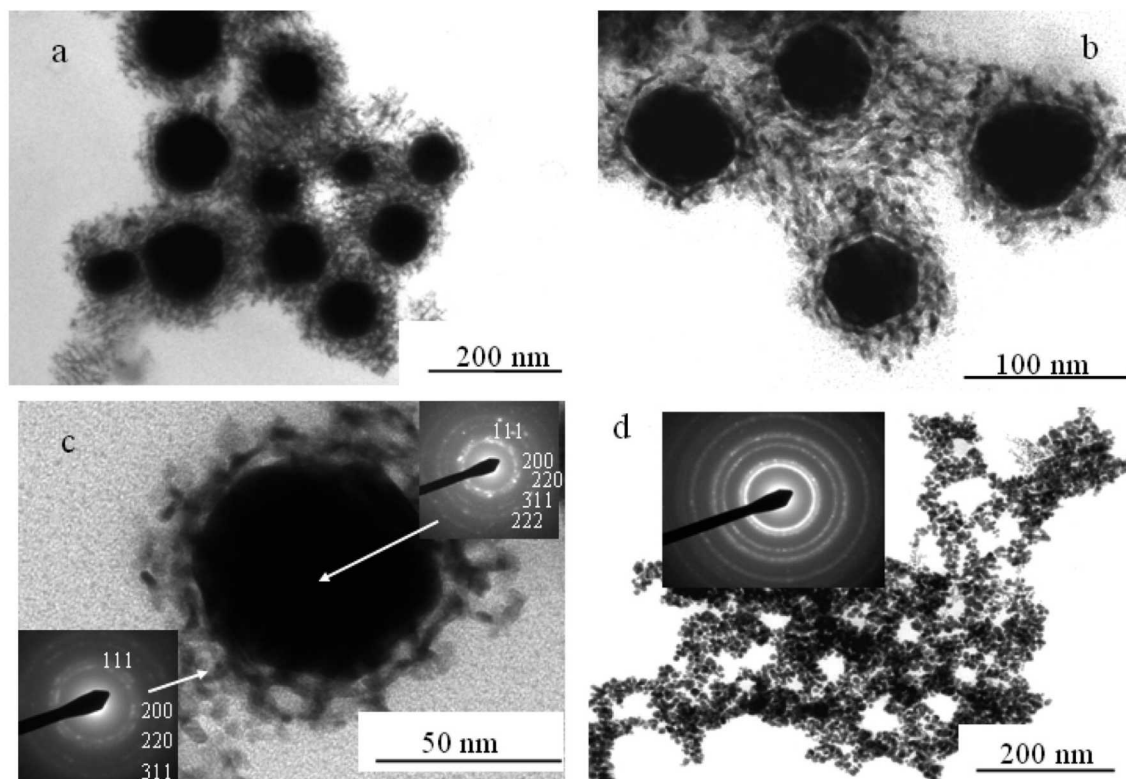


**Figure 1:** TEM images of Au-Pd NPs formed by  $\gamma$  -radiation (a, b and c) as core-shell nanoparticles formed by a gold dense core and a palladium porous shell and (d) as alloyed Au-Pt nanoparticles. Reprinted with permission from Chem. Mater. 2009, 21, 3677–3683. Copyright 2009 American Chemical Society.

### 3.1.2 Superalloys synthesis

Superalloys NPs are targeted phases for radiolysis synthesis. They are high temperature, corrosion resistant inorganic materials with both defense and civilian applications. The

addition of refractory elements to the traditional Ni based systems “hardens” the material to even higher temperatures, while retaining their superb mechanical strength. Traditionally, alloys are synthesized by a variety of methods including melt casting and sintering. Sintering is the preferred method (as compared to melting) as it will not destroy the refractories. It is anticipated that the radiolysis process will result in more defect-free superalloy due to the homogeneity of the NPs and the low temperature of both synthesis and sintering, thereby allowing for more energy efficient (lower process temperatures) and wider ranges of alloy compositions to be synthesized.

Recent research has focused on the use of radiolysis to synthesize superalloy NPs at room temperature. One example is with Co-Ni NPs. Using the methodology detailed earlier,<sup>23,82</sup> for the Co<sub>0.5</sub>-Ni<sub>0.5</sub> (50% Co and 50% Ni) alloy preparation, a 50 mL aqueous solution containing  $1 \times 10^{-4}$  M CoCl<sub>2</sub>,  $1 \times 10^{-4}$  M NiSO<sub>4</sub>,  $3 \times 10^{-4}$  M sodium citrate, 0.5 M methanol, and  $1.5 \times 10^{-2}$  M PVA, (M<sub>w</sub>, 88,000) was irradiated at a dose rate of 435 rad/s for 36 min. Synthesis and characterization results indicated homogenous nanoparticle formation, with NPs in the size range of 3-5 nm, in which each nanoparticle is shown to have a mixed composition of Co and Ni atoms; there is no evidence of core-shell nanoparticle formation. However, due to the small NP size lattice spacings from HRTEM could not be obtained. EDX analysis shows an approximate NP composition of 30% Co and 70% Ni. Furthermore, single particle elemental analysis data do indicate that individual NPs contain both Ni and Co, with an approximate elemental distribution of 28% Co and 72% Ni (as supported by broad range EDS). This composition is obviously different than the reactant mixture composition. At this point, there is no clear evidence if the composition is an approximation due to the small particle size being analyzed and the high resulting background count, or if not all the metal ions were reduced in the experimental time allotted.

### 3.1.3 Nanoparticle Sintering

The ability to sinter alloy NPs with minimal growth of defect sites is of great interest for bulk alloy applications, such as the use of superalloys in high temperature refractory engines and turbines.<sup>83</sup> The sintering of NPs can be achieved at temperatures much lower than required for coarse powders of the same materials. In general, the melting points of

nanoparticles are less than half of those of their corresponding bulk materials; sintering occurs at about two-thirds of suppressed melting temperatures, since the surfaces of nanoparticles have melting points that are lower than those of their cores. For example, NP sintering has been achieved through  $e^-$  beams<sup>84</sup> and microwaves<sup>85</sup> along with other room temperature techniques.<sup>86,87</sup> NP densification, sintering and grain-growth<sup>88</sup> is currently being studied by in-situ TEM.<sup>89,90</sup>

One example of this is the work on 50/50 AgNi NPs (Figure 2). This work was performed on a heated-stage TEM to reveal sintering temperatures and mechanisms. Equipment used included a JEOL 2010F field emission electron microscope in a bright field imaging mode at 200kV and a Gatan model 652 heating stage (range 25 – 800 °C). NPs were deposited from solution onto a Ti grid, and heated from RT to 800 °C. Small scale ripening occurs slowly ( $\approx$ 25 min) from RT to 450°C. However, from 450 – 800 °C, rapid large scale sintering occurs in the NPs. The NPs grow to a size of  $\approx$  100-150 nm. Figure 2 shows sizes of NPs at 450 and 800 °C.<sup>23,91</sup>

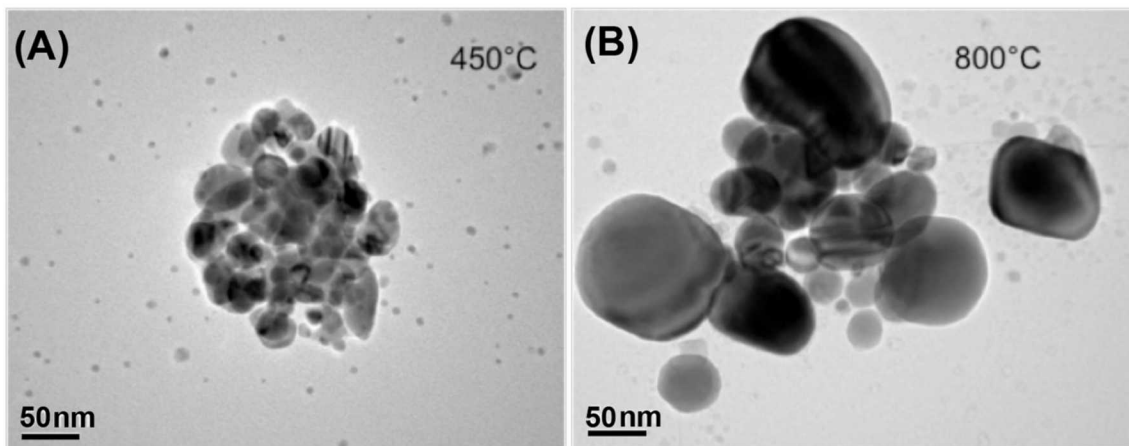


**Figure 2.** Sintering of Ag-Ni NPs on heated Transmission electron microscopy stage to (A) 450 °C and (B) 800 °C. Reprinted with permission from SAND2009-6424. Copyright (2009) Sandia National Laboratories.

TEM-EDS has also been used as a method to monitor the effects of temperature on nanoparticles formed by radiolysis. With the use of an in-situ heating stage on the TEM, Nenoff *et al.* were able to both confirm the crystal structure phase of  $UO_2$  formed under

varying pH conditions at room temperature by  $\gamma$ -irradiation.<sup>47,92</sup> Temperatures were stepped from RT to the predetermined temperature, held for 30 s, and stepped back to RT, successively, to 200 °C, 300 °C, 400 °C, 400 °C, 500 °C, 500 °C, and 600 °C; high resolution TEM, EDS and electron diffraction were carried out between heat treatments. The thermal stability of the UO<sub>2</sub> phase and the sintering behavior with respect to particle size and temperature were also monitored. As was reported, due to the uniform and nanosized nanoparticles with high surface area to volume ratio, the UO<sub>2</sub> sintered in the range of 500-600 °C, which is lower in comparison to bulk UO<sub>2</sub> sintered in the range 700-1000 °C.

### 3.1.4 Supported NPs and alloy

The radiolytic formation of metal nanoparticles in presence of support (organic or inorganic) is for long time a proved strategy to limit the coalescence of the nuclei with no need of additional organic modifiers such as surfactant at the surface of the NPs.<sup>19</sup> In this approach, the support can play the role of a matrix to limit the size of the NPs due to strong spatial hindrance, like in micro-mesoporous materials<sup>93-96</sup> or organics mesophase,<sup>97</sup> or to create directed 3D assembly, like by using micelles,<sup>98</sup> for example. In addition, the support plays an important role in the integration of the NPs into functionalized materials. To obtain NPs dispersed in the volume of the reaction, often a porous framework is used as a catalyst, or as a support on which the catalyst is fixed. Room temperature radiolysis can be used for the synthesis of both highly monodisperse nanoparticles in solution, and of nanoparticles on porous supports (such as polymers, metals, or metal oxide supports).

**Carbon support:** Nanoparticles (NPs) have been immobilized on a variety of carbon supports including mesoporous carbon, nanofibers, nanotubes, aerogels and xerogels, etc. All these supports are applied to achieve high dispersion, extensive electron transfer, and reduced agglomeration. The strong interaction between the catalyst and carbon support plays a significant role in the oxidation reaction.

Creative methods of synthesizing metal NPs via radiolysis enable their use in a wide range of supports, including polymers and aerogels. For example, the in-situ formation of silver

NPs in a polymer membrane by infiltrating a polymer matrix with silver ions has been achieved by Belloni et al.<sup>99</sup> The matrix is swollen with an appropriate solvent, followed by radiolysis inducing the NPs formation. The diffusion of ions is limited by the polymer matrix, and subsequent irradiation of the ions resulted in NP aggregates that are much smaller than those achieved in free solvent. When the polymer is de-swelled, porous polymer framework is infiltrated with NPs. Au and Ag NPs formed in aerogels have also been radiolytically prepared, showing further versatility of supports on which NPs may be deposited.<sup>100</sup> For example, aerogel supports for metal clusters are promising for varied applications in catalysis and sensors.

Bi-metallic clusters (Pt–Ru) on carbon supports (single- and multi- walled carbon nanotubes) using  $\gamma$ -ray irradiation were reported by Oh et al.<sup>101,102</sup> The aggregation of these bi-metallic nanoparticles was controlled by modifying the surface of the carbon (hydrophobic vs. hydrophilic) with conductive polymers (polyaniline, polypyrrole, and polythiophene).<sup>103</sup> Other bi-metallic clusters Pt–M (M = Ru, Ni, Co, Sn, and Au) were prepared by one-step gamma-irradiation. Further, functional polymers (poly(vinylphenyl boronic acid) and poly(vinylpyrrolidone) were used to anchor these Pt–M nanoparticles on multi- walled carbon nanotubes using gamma- irradiation in aqueous solution at room temperature.<sup>104</sup> These materials were promising for direct methanol fuel cell electrode production. Another bimetallic clusters such as Co–Pd or Ni–Pt with strong magnetic susceptibility and high magneto-anisotropy were prepared as well.<sup>2</sup>

Conducting polymers such as poly(3,4-ethylenedioxythiophene), polyaniline, and polypyrrole have been also employed as carbon supports with unique p-conjugated structures, high electrical conductivities, and exceptional environmental stabilities.<sup>105,106</sup> Pt–Ru and Pt–Sn binary catalysts supported on polyaniline have been reported.<sup>107</sup> Multilayered Pt/CeO<sub>2</sub> and ZnO/Pt/CeO<sub>2</sub> on polyaniline as hybrid hollow nanorod arrays were developed; these hybrids provide short diffusion paths for electroactive species and demonstrate elevated electrocatalytic activity.<sup>108</sup>

Pt–Ru NPs were formed on polymer coated multi walled carbon nanotubes (MWNT).<sup>109</sup>

Hence, radiolytic methods were applied to prepare metal NPs at the surface of textile for antibacterials effects.<sup>110</sup> Besides, in view of photocatalytic applications monometallic and bimetallic NPs were synthesized at the surface of  $\text{TiO}_2$  by gamma-radiolysis, such as Ag,<sup>111</sup> Au-Cu,<sup>112</sup> Ni-Au.<sup>113</sup> Multi-walled carbon nanotubes were also investigated as a support for Ni.<sup>114</sup> Pt-Zn alloy were prepared on  $\text{ZnO}$  by irradiation using the TEM electron beam.<sup>70</sup> Metals (Pt, Au, Cu or Ni) nanoparticles supported on iron oxides were prepared via radiolysis technique using a 4.8<sup>-</sup> MeV electron beam.<sup>115</sup>

A radiochemical approach for the synthesis of bimetallic (PtPd) and trimetallic (PtPdAu) catalysts supported on polypyrrole nanofibers without using reducing agents was presented recently (Figure 3).<sup>116,117</sup> Au(III) acetate, Pt(II) and Pd(II) acetylacetone and Ppy nanofibers were used as precursors. The synergistic effect of the redox-rich properties of the polymer and the catalytic activity of the metal nanoparticles make them suitable for the electro-oxidation of methanol. The uniform dispersion of bimetallic and trimetallic NPs leaded to superior mass activity, stability for methanol oxidation, and lower metals loading which decreases the cost of the catalyst.

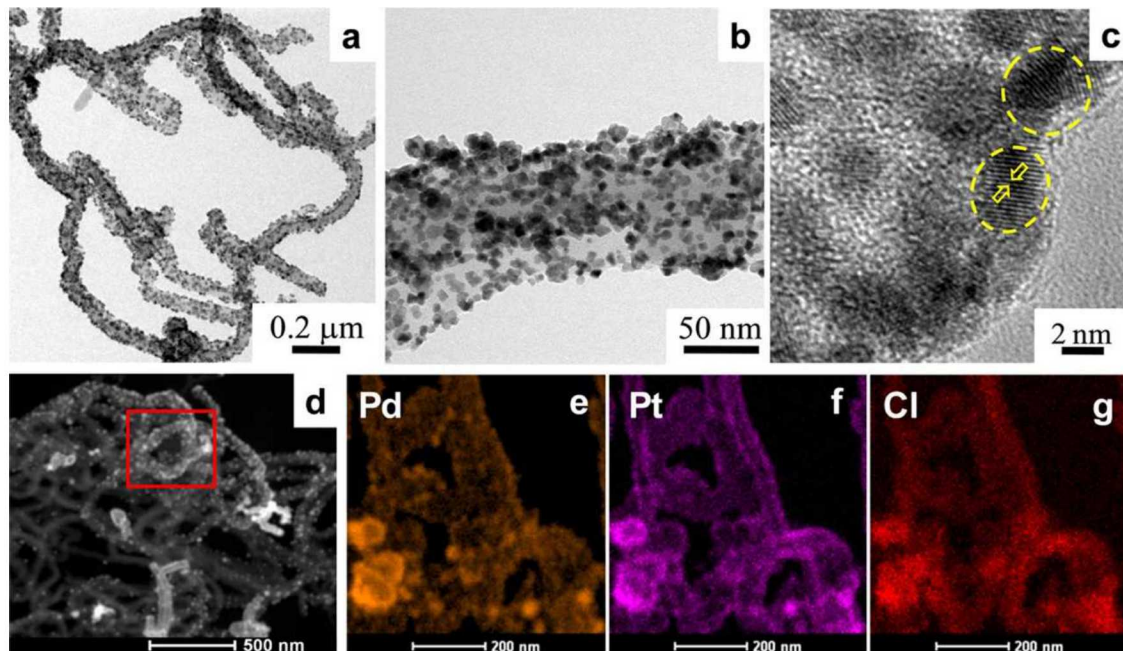


**Figure 3:** TEM images of (a-b)  $\text{Pd}_{89}\text{Pt}_{11}/\text{Ppy}$  nanohybrids at different magnifications, (c) HRTEM of  $\text{Pd}_{89}\text{Pt}_{11}/\text{Ppy}$ , (d) HAADF-STEM image of  $\text{Pd}_{89}\text{Pt}_{11}/\text{Ppy}$  nanohybrids. (e-g) HAADF-STEM-EDS mapping images of  $\text{Pd}_{89}\text{Pt}_{11}/\text{Ppy}$  showing elemental distribution of

Pd, Pt and Cl, respectively. Reprinted with permission from ACS Appl. Mater. Interfaces, 2017, 9, 33775–33790. Copyright (2017) American Chemical Society.

**Amorphous Silica:** Lehoux et al. developed oil-swollen hexagonal mesophases as supports for metallic salts, which were used as soft templates for radiolytic synthesis of 3D bimetallic Pd-Pt alloyed nanostructures.<sup>118</sup> The authors demonstrated that the formation of alloys can be controlled by a slow and homogeneous reduction of the mesophases by  $\gamma$ -irradiation under mild conditions (irradiation dose of 91.2 kGy for 48 h). The soft templating technique leads to a tunable three-dimensional porosity and influence on the composition of the Pt-Pd nanostructures.

Nanoalloyed clusters (Ni–Pt) on amorphous silica ( $\text{SiO}_2$ ) were synthesized by radiolysis.<sup>119,120</sup> The amount of Pt was varied stepwise (2, 9, 15, 25, 35, 85 and 95 at.%), and radiolytic process was carried at RT. The size, structure and magnetization of the Ni–Pt nanoparticles were controlled by the radiolytic conditions. It was demonstrated that Pt had a major role on the magnetization at low temperature by enhancing the nickel ion reduction and protecting Ni against corrosion during the synthesis. The specific magnetization enhancement at low temperature of the Ni–Pt/ $\text{SiO}_2$  was explained with the small size and a narrow cluster size distribution of magnetic domains. Alloying of Ni with Pt favors the nickel reduction yield and enhances the magnetization of the Ni–Pt clusters.

**Carbon and Silica Supports:** Gamma irradiation was applied to load CoPd bimetallic particles onto MWNT in the presence of silica.<sup>121</sup>

**Graphene oxide:** Bimetallic  $\text{Au}_{90}\text{Pd}_{10}$  and trimetallic  $\text{Au}_{50}\text{Pd}_{25}\text{Pt}_{25}$  materials with high electrocatalytic performance for glucose in alkaline medium were prepared on graphene oxide (GO) or reduced GO (rGO) by radiolysis.<sup>122</sup> Stable Au with active Pd and Pt NPs on graphene nanosheets (GO) were combined and thus alloys of  $\text{Au}_{90}\text{Pd}_{10}/\text{rGO}$  and  $\text{Au}_{50}\text{Pd}_{25}\text{Pt}_{25}/\text{rGO}$  were prepared. The morphologies of the GO had an effect on the alloys (GO is more stacking of sheets and rGO is with separated flake and fold structure). The advances in the use of rGO as a more efficient anode material for the electrochemical

energy conversion and storage applications are demonstrated.

**Zeolites:** Among different supports, zeolites constitute an important class of materials due to their ion-exchange capacity that permits controlled incorporation and immobilization of metal cations. Besides, the large variety of 3D and 2D framework structures can be used as a hard template to control the properties of the NPs. Zeolites are recognized as appropriate materials for stabilization of small metal NPs and clusters, notably formed by radiolysis.<sup>93,94</sup> However, unlike for the synthesis of NPs in solution, the radiation beam is now interacting directly with the zeolite, and the radiation subsequently modify the chemistry.<sup>123,124</sup> In addition, the accessibility inside the porous volume limits the application of the chemical methods developed in solution in order to control the reduction conditions. And finally, due to the high-concentration of metal cations in the matrix, high dose of irradiation must be applied in order to achieve the reduction of a significant part of the ion-exchanged cations. Alternatively to the direct irradiation of micrometer-sized zeolite crystals, the zeolite nanocrystals can be stabilized in colloidal suspensions and subjected to direct irradiation (Figure 4). Indeed, colloidal suspension of nanozeolites contains less than a few percent in mass of crystals that are homogeneously distributed through the volume of the aqueous solution. In these favorable conditions, the irradiation beam interacts with the aqueous phase to generate the reducing radiolytic species, and notably, the solvated electrons ( $e^-_{aq}$ ), that by diffusion reach the metal cations. Pulse radiolysis measurements demonstrated the efficient scavenging of the  $e^-_{aq}$  by  $Ag^+$  cations supported on BEA zeolite nanocrystals.<sup>125</sup> The gamma-radiolysis approach was also applied to prepare Cu,<sup>41,126</sup> Pd, and Pt NPs in nanosized zeolites with various frameworks.<sup>127,128</sup> The size, distribution and nature of the NPs were controlled by the irradiation dose, type of zeolite framework and metal content. For example, Cu with selective oxidation states of  $Cu^0$  and  $Cu^1$ ,<sup>126</sup> and small clusters in the GIS-type zeolite were prepared by gamma radiolysis of zeolite colloidal suspension, in presence of isopropanol.<sup>41</sup> Alloy NPs (AuAg, PdAg, PtAg, PdPt) with controlled size (2–10 nm) and composition were encapsulated in silicalite-1 single zeolite nanoboxes using the classical HT treatment.<sup>129</sup> The zeolite nanoboxes act as protective microporous shell preventing the NPs from sintering by coalescence.

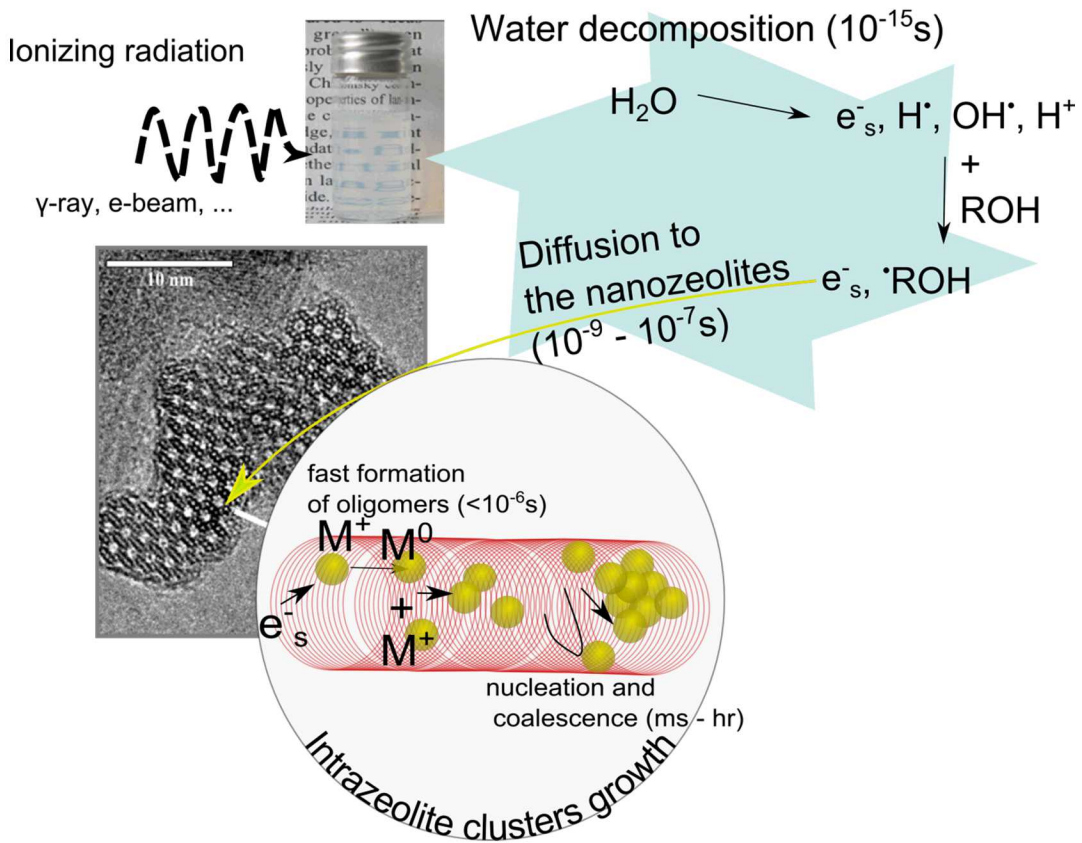


**Figure 4:** Elementary processes and time-scales governing the formation of metal and alloy nanoparticles in colloidal suspensions of zeolite nanocrystals.

### 3.2 Characterization Techniques

Nanoalloy synthesis by radiolysis typically produces uniform NPs with small diameters of less than 5 nm. Due to the small size of the nanoparticles, often a variety of characterization techniques are employed to both fully characterize the nanoparticles and to understand the structure-property relationship of the NPs with their application. Techniques commonly employed include transmission electron microscopy (TEM), X-ray spectroscopy, and optical spectroscopy.

The TEM techniques include high-resolution transmission electron microscopy (HRTEM) which allows for lattice determination of NPs; one example of HRTEM with nanoalloys is in the U-La phase space.<sup>47</sup> Furthermore scanning transmission electron microscopy

(STEM) can be combined with high angle annular dark field (HAADF), which allows for Z contrast to distinguish between elements combined with lattice information of the NPs. This further confirms alloying in the nanoparticle; an example is the study of nanoalloys in the Ag-Ni phase space.<sup>23</sup> (see Figure 5)

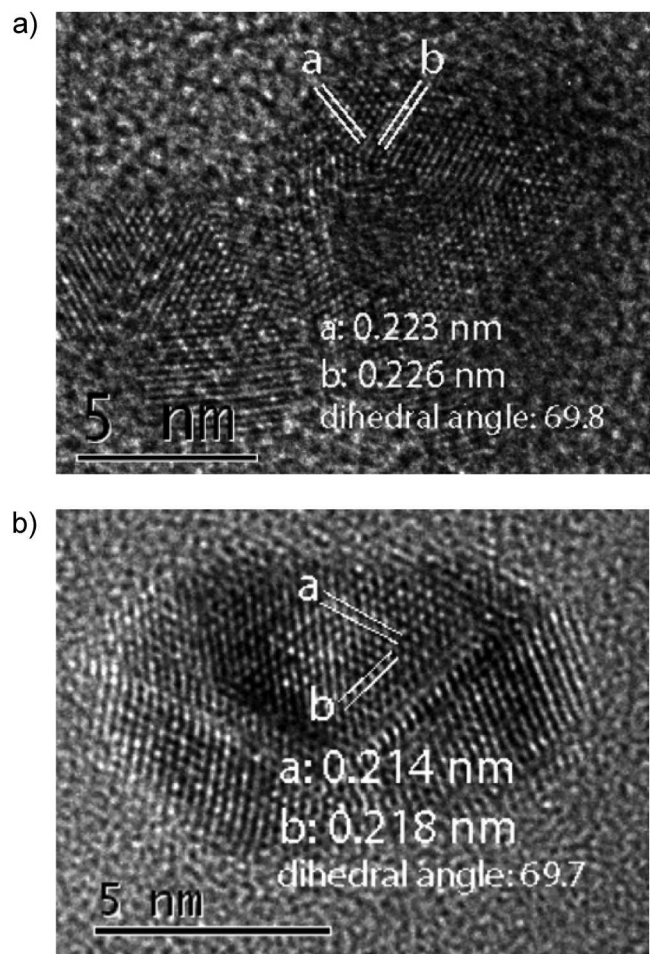


**Figure 5:** Transmission electron microscopy images of (A) HRTEM image of Ag-Ni nanoalloys. In the image, a) is 0.223 nm, b) is 0.226 nm, and the dihedral angle between a and b is 69.8°. For lattice spacing, Ni (111) 0.203 nm, Ag (111) 0.236 nm, and prediction from Vegard's law for 50% Ag and 50% Ni is 0.220 nm. (B) HRTEM image of a Pd0.5-Ni0.5 alloy nanoparticle. In this image, a) 0.214 nm, b) 0.218 nm, and the dihedral angle between a and b is 69.7°. For lattice spacing, Ni(111) 0.203 nm, Pd(111) 0.225 nm, and the prediction from Vegard's law for 50% Pd and 50% Ni is 0.214 nm. Reprinted from J. Phys. Chem. C, 114, Z. Zhang, Room-Temperature Synthesis of Ag-Ni and Pd-Ni Alloy Nanoparticles; 14309-14318, Copyright (2010) with permission from American Chemical Society.

X-ray spectroscopy techniques, including X-ray adsorption spectroscopy (XAS) and X-ray photoelectron spectroscopy (XPS), are used to provide NP elemental information. Chemical composition, such as relative concentration of various elements in a bimetallic NP can be determined by techniques such as Energy-dispersive X-ray. Optical spectroscopy is utilized to understand bulk characteristics of the NPs. In particular, ultraviolet visible (UV-Vis) spectroscopy allows for the study of chemical compositions and light scattering for determining NP size, size distribution and aggregation behavior during nanoparticle cluster formation.

Pulse radiolysis has been successfully used to study the formation mechanisms of monometallic species<sup>130</sup> and of nanometer scaled clusters and the reactivity of those clusters in solution to form nanoparticles.<sup>62,63,64</sup> The group of Hastings observed a relationship between solution and deposit compositions of bimetallic nanoparticles using electron-beam induced deposition technique.<sup>131</sup> Interestingly, they suggest that pulse radiolysis studies might be useful to predict the deposit composition.

### 3.3 Reaction mechanisms

For both a fundamental understanding of the science governing NP formation via radiolysis and as a method for producing NP compositions by design, mechanistic studies are acknowledged to be vital to the field of research. The following is the general theory that has been derived for both core/shell and nanoalloy formations via radiolysis.

#### 3.3.1 NPs formation under radiolysis.

The radiolysis of aqueous solutions by gamma rays can produce oxidizing and reducing agents of exceptional potency: creates hydrated electrons, H atoms and hydroxyl radicals. Alcohol molecule are generally used to scavenge H atoms (H<sup>•</sup>) and hydroxyl (OH<sup>•</sup>) radicals. For example, in case of methanol (Eq. 1), the yield of hydroxymethyl radicals (·CH<sub>2</sub>OH) is 4.4/100eV, if oxidation from H<sub>2</sub>O<sub>2</sub> is considered.<sup>132,133</sup>



The redox potentials of hydrated electrons and hydroxymethyl radicals ( $\text{CH}_2\text{OH}$ ) are -2.7 V<sup>134</sup> and -1.18 V,<sup>135</sup> respectively. The hydrated electrons and formed hydroxymethyl radicals reduce the metal salts in solution to produce nanoalloys. During the irradiation, the concentrations of the reactive species in the solution evolve at a rate determined by solution pH and the concentrations of dissolved gases.

### **3.3.2 NP nuclei formation stage.**

The formation of NPs involves two stages, nucleation (relatively fast process associated with the formation of the first oligomeric species by reduction and coalescence) and growth (relatively slow process involving the reduction at the surface of the formed nuclei)<sup>136,137</sup> The nucleation process induced by irradiation determined the alloy or core-shell nature of the NP (Figure 6), At high dose rate, the hydrated electrons reduce a sufficient high concentrated in both metal atoms to generate nanoalloy clusters, which may have a diameter of less than 1 nm and are the nuclei for particle growth.<sup>23,136</sup> Whereas at low dose rate, in the case of more than one metal, clusters of each individual metal and core-shell metal will be formed. Nanoalloy vs core-shell NPs formation is due to kinetic competition, involving an intermetallic electron transfer quench mechanism as shown in Figure 6.

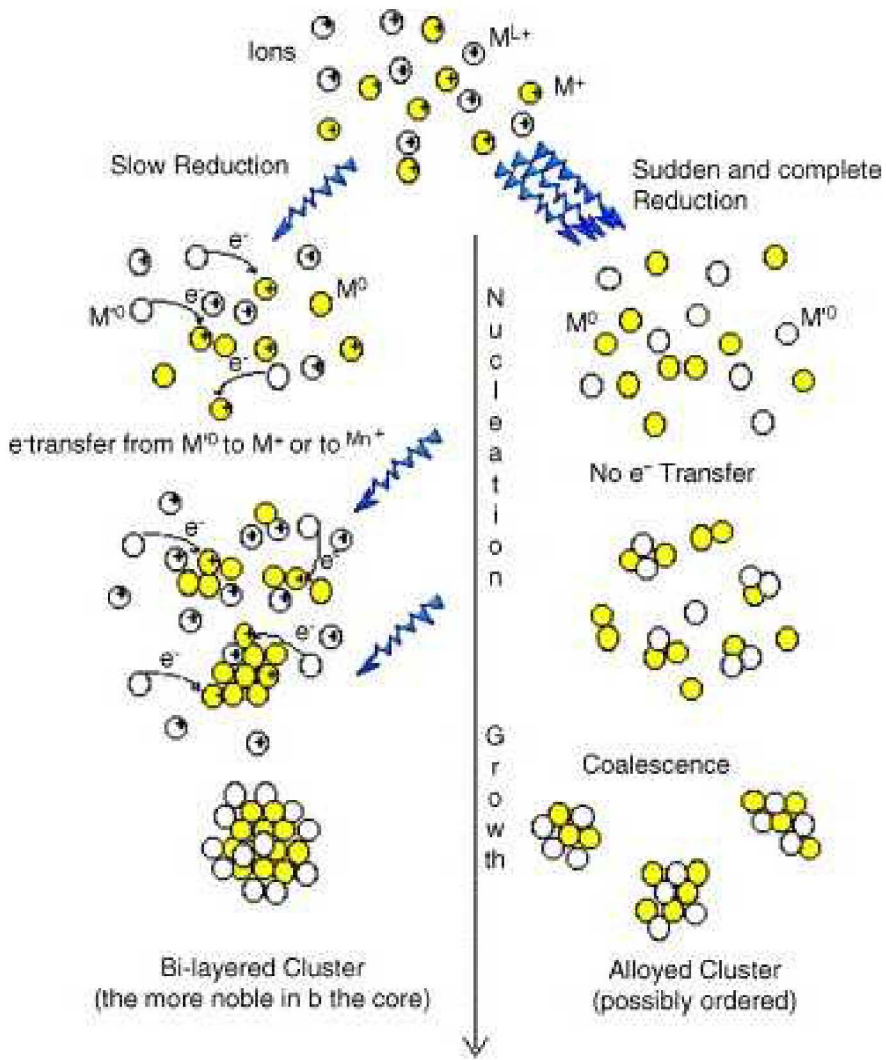


**Figure 6:** Schematic illustration of the nucleation and growth which occur under low (left) or dose (right) dose rate reduction conditions. Reprinted from Catal. Today, 113, J. Belloni, Nucleation, growth and properties of nanoclusters studied by radiation chemistry Application to catalysis, 141-156, Copyright (2006), with permission from Elsevier.

Low dose rate and high dose rate are determined relative to the speed at which the reduced metal ions will transfer electrons from the less noble metal to the more noble metal. Some alloys, such as Au-Pt have not been demonstrated to alloy using radiolysis, presumably due to their rapid electron transfer caused, in part, by the multivalent ions,<sup>32</sup> whereas such bimetallic species as Cu-Pd and Pt-Ag will alloy even at relatively low dose rates compared to other bimetallics.<sup>2</sup>

### 3.3.3 Nanoalloy NP growth stage.

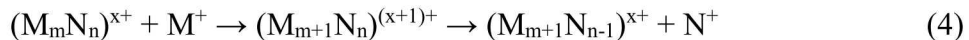
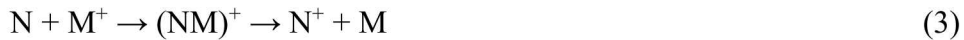
After nanoalloy cluster nuclei are formed, a nanoparticle growth stage begins. For the growth stage, radicals can transfer electrons to nuclei or small metallic particles and form an “electron pool” on nuclei or small particles.<sup>132,138</sup> In certain nanoalloy examples,<sup>1,23</sup> there is a transfer of electrons to the tiny bimetallic nuclei clusters from the hydroxymethyl radicals ( $\cdot\text{CH}_2\text{OH}$ ) resulting in the generation of electron pools (Eq. 2), similar to the case of Pd NP formation.<sup>139</sup> Ions in solution accept electrons from the charged nanoalloy clusters and cause new ions to reduce onto the surface of these clusters. Such a growth process for nanoalloy clusters (generically labeled:  $(\text{NM})_x$ ) finally leads to the formation of nanoalloy NPs (see Eq. 2). Hydrogen formation by stored electrons in nanoalloy clusters and radical-radical reactions can be the competing reaction of the above growth process.<sup>43</sup> However, these reactions do not have a significant effect on particle formation as confirmed by experiments and calculations.<sup>132</sup>



Similar to earlier reports on NP alloy formation by radiolysis,<sup>23,38,82</sup> high dose rates reduce the N and M ions within a very short time, shorter than any other electrochemical or thermodynamic process. Therefore, it can mostly suppress the possible intermetallic electron transfer between the two ions or atoms. High dose rates result in the formation of an alloy structure, which has the same metal ratio as their ionic precursors because both metal atoms are quenched suddenly into the lattice. The intermetallic electron transfer quench mechanism also occurs in the two stages, nucleation and growth, and is complimentary to the whole particle formation process from the kinetic aspect. Such a mechanism explains that kinetically favored alloy structure can be formed with a very fast reducing rate.

This theory has been confirmed by a number of researchers,<sup>23, 82, 140</sup> the first of which was Belloni et al.<sup>1</sup> The group used  $\gamma$ -irradiation method to synthesize bimetallic Au-Ag NPs and studied the structures of these particles with different dose rates.<sup>38</sup> (Au and Ag are miscible at any ratio, as documented in the binary phase diagrams.<sup>141</sup>) They found that, at

a low dose rate (either 0.25 or 3.8 kGy/h, which equals 6.9 or 106 rad/s, respectively), the less noble metal ions (i.e. “M” = Ag) act as an electron relay towards the more noble metal ions (i.e., “N” = Au), Eq. 3 and 4. Thus, monometallic clusters  $Au_m$  are formed first and then, when Au ions are exhausted,  $Ag^+$  ions are reduced afterwards at the surface of  $Au_m$ , where N is less noble metal (e.g. Ag) and M is more noble metal (e.g. Au).



The final result is a core-shell cluster where the more noble metal Au is coated by the less noble metal Ag.

However, high dose rates (35 kGy/h, i.e., 972 rad/s) practically block intermetallic electron transfer between noble core metals and the less noble metal ions in solution. As a result, there is a sudden reduction of all metal ions in solution that makes the charge transfer between more noble ions (e. g.,  $Au^+$ ) and less noble atoms (e. g., Ag) impossible. This results in the formation of only homogenous Au-Ag nanoalloy nanoparticles.<sup>32,38</sup>

Interestingly, this high dose radiolysis method is also a way of creating homogenous nanoalloys of phases predicted to be immiscible via thermodynamic reaction mechanisms. One example is the case of Ag-Ni NPs. Utilizing similar reaction conditions as those used for the radiolysis formation of Au-Ag nanoalloys, an aqueous solution of silver and nickel salts was combined with methanol, the capping agent sodium citrate, and a stabilizing agent poly vinyl alcohol, and irradiated at a dose rate of 300 rad/s (10.8 KGy/h) for 18 min. This corresponds to approximately five times the dose required for total reduction of  $Ag^+$  and  $Ni^{2+}$ . The  $\gamma$ -irradiation creates hydrated electrons, H atoms, and hydroxyl radicals from the water. All evidence indicates that  $Ag^+$  and  $Ni^{2+}$  were reduced by these two reducing species to form Ag-Ni nanoalloys.

Confirmation of metal reduction mechanisms to form nanoalloys is performed by analysis of the redox potentials of the metal ions in solution as compared to the reducing potential of the radicals in solutions. The redox potentials of  $Ag^0$  (Ag atom and bulk) are calculated to be -1.8 V<sup>142</sup> and 0.8 V, respectively. Other reports indicate the redox potential for  $Ag^+$

to  $\text{Ag}^0$  atom is -2.1V.<sup>143,144</sup> Therefore, it is expected that it is difficult for hydroxymethyl radicals ( $\text{CH}_2\text{OH}$ , -1.18 V) to reduce  $\text{Ag}^+$  to  $\text{Ag}^0$  atom in the absence of NPs, due to the very negative potential of  $\text{Ag}^0$  (-2.1 V). The redox potentials of  $\text{Ni}^0$ ,  $\text{Ni}^{2+}$ , and  $\text{Ni}^+$  are -2.2,<sup>145</sup> -1.05 to -1.28 V, and -1.7 V, respectively. This suggests that it may be possible for  $\text{Ni}^{2+}$  reduction to occur in the presence of organic radical anions such as  $\text{CH}_2\text{OH}$ , electron scavengers, and hydrogen atoms, not just hydrated electrons.

Therefore,  $\text{Ag}^+$  and  $\text{Ni}^{2+}$  are almost solely reduced by hydrated electrons at the very beginning of the reaction. Similar to the case of  $\text{Ag}$ ,<sup>146</sup> hydrated electrons generate  $(\text{AgNi})_x$  alloy clusters, which may have a diameter of less than 1 nm and are the nuclei for particle growth.  $(\text{AgNi})_x$  formation from high dose rates is due to kinetic competition, that is, an intermetallic electron transfer quench mechanism. The competing reaction of this growth process is hydrogen formation by stored electrons in clusters.<sup>132</sup>

### 3.4 Catalysis and further applications

From the late 1980's, there has been growing, and sustained, interest in "small particles," "clusters," or nanoparticles.<sup>27</sup> Early findings of unique electronic, optical, chemical and magnetic properties in small particles compared to that of the bulk spurred growth in the field of nanoparticle synthesis, characterization, and ultimately applications. Because NP formation by radiolysis occurs at room temperature, adverse thermal effects on NP preparation and subsequent applications are avoided. This includes thermal effects on stoichiometry of the NP, phase degradation of support material (eg., zeolites, oxides, etc), morphology of NP, and core/shell vs. homogenous nanoalloy composition. Applications of metallic, alloy and oxide NPs are strongly dominated by those taking advantage of their extremely high surface to volume ratio, enabling small volumes of high value materials like Au and Ag to efficiently act as catalysts. Catalysis is a dominant area of focus for NPs,<sup>147</sup> while ventures into their use in coatings, electrodes and sensors have also been pursued.<sup>3,11</sup> among other diverse applications such as magnetism or biomedicine.<sup>148</sup> Concerning magnetism, one example has been reported by the group of Belloni in which they demonstrated that radiation-induced NiPt supported on  $\text{SiO}_2$  have improved magnetic

properties at low temperature.<sup>120</sup> In addition the authors observed that increasing the Pt content of the nanostructure leads to an increase of its magnetization.

Below a number of applications that have been explored for nanoalloys synthesized via radiolysis is described. Although not an exhaustive list, this section is meant to give the reader a general idea of the broad applicability of the radiolysis method in materials production.

While radiolysis is only one of many techniques amenable to forming commonly synthesized metallic NPs such as Ag, Au, Pt and Pd; radiolysis is uniquely suited for the synthesis of such NPs on a range of supports (see above supported synthesis), which are important for catalytic applications. The high surface to volume ratio of well-dispersed metallic NPs allows for increased catalytic yield in a smaller volume over techniques in which aggregation is more prevalent.

Catalysis in the field of energy has been extended to hydrogen synthesis, and to catalysts for fuel cells. Catalysts for fuel cell technology<sup>149</sup> such as Pt NPs on carbon serve to reduce oxygen for use in fuel cells. Related work on alloyed Pt NPs as potential electrocatalysts in fuel cells (when attached to carbon supports) has also been reported.<sup>150</sup> These Pt NPs are formed radiolytically, and used in conjunction with the anodes and cathodes of fuel cells to facilitate the electrocatalytic reaction for energy conversion. Ksar et al. reported that radiolytic synthesis of Pd-Au core-shell nanostructures in mesoporous phases are more stable than the one in solution for application in direct ethanol fuel cells.<sup>81</sup> Recently, bi-(Pt-Pd, Pd-Au) and tri-metallic (Pt-Pd-Au) supported on nanofibers of different compositions demonstrated a noticeable enhancement of the catalytic activity and stability for methanol and ethanol oxidation reactions.<sup>116,117</sup> Those metals/polymer hybrid materials have been prepared via radiolysis route.

Numerous methods for hydrogen production using metallic NP catalysts by radiolysis are ongoing. This research is of importance in identifying the most efficient and cost effective method of hydrogen production for large-scale applications. Meisel and coworkers have done extensive work in the area of hydrogen production through catalysis: they have shown that by radiolytically forming gold microspheres, they can form hydrogen;<sup>151</sup> their work

with Au NPs serve to catalyze hydrogen production; and their Ag NPs catalysts is used to form H<sub>2</sub> also under radiolysis.<sup>152</sup> Hydrogen has also been formed from formaldehyde.<sup>153</sup> Supported bimetallic NPs on TiO<sub>2</sub> are found efficient for hydrogen production via photocatalysis.<sup>112,113</sup>

Catalysis in waste remediation is proving to be an important area of research. Au NPs were deposited on high surface area magnesium oxide using vacuum-UV laser ablation leading to improved stability of the Au NPs on the support. The supported Au NPs efficiently catalyzed the decomposition of various volatile organic compounds, nitrogen oxide and sulfur oxide compounds at room temperature, thus reducing pollutants in air.<sup>154</sup> NPs for use in environmental remediation is a promising field, not only for remediation but for sensing as well, to identify contaminants. In addition, the oxidation of toxic substances for their degradation, through a combination of semiconducting NPs with UV irradiation has been reported.<sup>155</sup> Metallic doped NPs such as Ni doped titania are being investigated in order to move the degradation chemistry to occur under visible light rather than the UV required with semiconductor materials.

The aggregation tendency of NPs at the support is a major problem for stable performance especially on catalysis, and hence, the use of conducting supports is essential for fabrication of active electrocatalysts. Graphene, graphene oxide (GO) and reduced GO (rGO) are important supports for achieving enhanced electrochemical performances.<sup>156</sup> The combination of rGO nanosheets with metal alloys showed the synergistic effect (Au<sub>90</sub>Pd<sub>10</sub>/rGO and Au<sub>50</sub>Pd<sub>25</sub>Pt<sub>25</sub>/rGO) and thus nanocomposites with excellent electrocatalytic activity and stability for glucose oxidation were prepared. This improvement of performance has been assigned to the specific structures of the nanocomposites enable a better interaction between the components, and by proceeding mostly in a 2-electron process leading to gluconate as the sole reaction product, thus highlighted the high selectivity.<sup>106</sup>

#### 4. Conclusions

Radiolysis, along with other radiation driven synthesis techniques, is being used to improve our understanding of NP formation and to expand the synthesis toolbox. This review is intended to inspire a growth in research on radiolysis as it applies to metallic nanoparticle formation. Potential exists for significant research contributions in the area of nanoalloys synthesis and development of related applications, in addition to more fundamental research using pulse radiolysis studies and modeling efforts to assist in understanding reaction mechanisms.

A wide variety of monometallic nanoparticles (NPs) and, more recently, bimetallic NPs have been synthesized using radiolysis from various techniques which employ ionizing radiation sources. Gamma radiation is the most common means by which ionizing radiation is employed to synthesize NPs. Gamma rays have low linear energy transfer, allowing for larger volumes of material to be irradiated, and therefore larger volumes of sample to be synthesized by a relatively easy technique, which does not rely on complex or expensive machinery. In addition, the dose rate can be readily calculated and is easily tunable by varying the distance of the sample from the source. In bimetallic nanoparticles, the radiation dose rate relates to the resulting nanoparticle structure. In general, at low dose rates core-shell NPs are formed, while at sufficiently high dose rates alloys can occur, even in mixtures for which alloying is not thermodynamically favored such as Ag-Ni nanoalloys. By altering dose and dose rate, in addition to precursor salt concentrations and the order in which precursors are reacted, the resulting NP structure can be tailored more precisely than with other synthesis techniques.

The growing list of bimetallic NPs and nanoalloys formed to date indicate that radiolysis may be used to discover other novel nanoalloys. However, in order to best approach the design of new NP alloys, it is important to further the understanding of reaction mechanisms leading to NPs nucleation and growth. Experimentally, pulse radiolysis has been important in the study of NPs formation mechanisms. Furthermore, theory and modeling efforts are promising complements to experimental work in the field of understanding NP synthesis by radiolysis. Modeling radiolysis-assisted NP growth is a subset of the fledging field of computational electrochemistry. Accurate redox potentials

and the free energy changes of nucleation in water need to be computed routinely using electronic structure methods. Specific to NPs growth is the need to bridge time- and length-scales between the initial stage of growth involving cluster size < 10 atoms, and later stages with >1000 atoms using more coarse-grained models.

Because the radiolysis technique employs synthesis in aqueous solution, near room temperature, a wide variety of applications can be accessed in addition to the wide variety of NPs that can be formed. The potential for applications is exciting because the way in which synthesis can occur within zeolite pores, on conductive polymer coated nanowires, or within varied polymer matrices can be envisaged. The ability to directly synthesize onto such a wide variety of supports gives a glimpse of the versatility of this technique in designing applications. Areas of interest for radiolysis-induced NP formation include continued focus on catalysts by designing alloys with improved selectivity for sensors, or improved catalytic properties. It may also be extended to the areas of medicine and energy. Additionally, the ease of NP production at relatively large-scale using radiolysis makes this technique a commercially viable avenue to forming NPs.

### **Acknowledgments:**

This work is supported by the Laboratory Directed Research and Development Program at Sandia National Laboratories. Sandia National Laboratories is a multimission laboratory managed and operated by National Technology and Engineering Solutions of Sandia, LLC, a wholly owned subsidiary of Honeywell International, Inc., for the U.S. Department of Energy's National Nuclear Security Administration under contract DE-NA0003525. This paper describes objective technical results and analysis. Any subjective views or opinions that might be expressed in the paper do not necessarily represent the views of the U.S. Department of Energy or the United States Government.

## References:

- (1) Belloni, J. Nucleation, growth and properties of nanoclusters studied by radiation chemistry Application to catalysis. *Catal. Today* **2006**, *113*, 141-156.
- (2) Ferrando, R.; Jellinek, J.; Johnston, R. L. Nanoalloys: From Theory to Applications of Alloy Clusters and Nanoparticles. *Chem. Rev.* **2008**, *108*, 845-910.
- (3) Munoz-Flores, B.; Kharisov, B. I.; Jimenez-Perez, V. M.; Martinez, P. E.; Lopez, S. T. Recent Advances in the Synthesis and Main Applications of Metallic Nanoalloys. *Ind. Eng. Chem. Res.* **2011**, *50*, 7705-7721.
- (4) Callister, W. D. Chapter 11: Applications and Processing of Metal Alloys in Materials Science and Engineering: An Introduction, 7<sup>th</sup> edition, Callister, W. D. Ed., John Wiley and Sons, Inc. New York **2007** 359.
- (5) Amendola, V.; Meneghetti, M.; Bakr, O. M.; Riello, P.; Polizzi, S.; Anjum, D. H.; Fiameni, S.; Arosio, P.; Orlando, T.; Fernandez, C. D. J.; et al. Coexistence of plasmonic and magnetic properties in Au<sub>89</sub>Fe<sub>11</sub> nanoalloys; *Nanoscale* **2013**, *110*, 5611-5619.
- (6) Stamenkovic, V. R.; Mun, B. S.; Arenz, M.; Mayrhofer, K. J. J.; Lucas, C. A.; Wang, G. F.; Ross, P. N.; Markovic, N. M. Trends in electrocatalysis on extended and nanoscale Pt-bimetallic alloy surfaces. *Nat. Mater.* **2007**, *6*, 241-247.
- (7) Huang, X.; Li, Y.; Li, Y.; Zhou, H.; Duan, X.; Huang, Y. Synthesis of PtPd bimetal nanocrystals with controllable shape, composition, and their tunable catalytic properties. *Nano Lett.* **2012**, *12*, 4265-4270.
- (8) Chen, G.; Desinan, S.; Rosei, R.; Rosei, F., Ma, D. Synthesis of Ni-Ru alloy nanoparticles and their high catalytic activity in dehydrogenation of ammonia borane. *Chem. Eur. J.* **2012**, *18*, 7925-7930.
- (9) Toshima, N.; Yonezawa, T. Bimetallic nanoparticles—novel materials for chemical and physical applications. *New J. Chem.* **1998**, *22*, 1179-1201.
- (10) Sárkány, A.; Hargittai, P.; Geszti, O. Thermal and radiolysis assisted formation of Au-Pd heteroaggregates. *Colloid. Surface. A* **2008**, *322*, 124-129.
- (11) Zaleska-Medynska, A.; Marchelek, M.; Diak, M.; Grabowska, E. Noblemetal-based bimetallic nanoparticles: the effect of the structure on the optical, catalytic and photocatalytic properties. *Adv. Colloid. Interface Sci.* **2016**, *229*, 80-107.
- (12) Narayanan, K. B.; Sakthivel, N. Biological synthesis of metal nanoparticles by microbes. *Adv. Colloid. Interface. Sci.* **2010**, *156*, 1-13.
- (13) Akita, T.; Hiroki, T.; Tanaka, S.; Kojima, T.; Kohyama, M.; Iwase, A.; Hori, F. Analytical TEM observation of Au-Pd nanoparticles prepared by sonochemical method. *Catal. Today* **2008**, *131*, 90-97.
- (14) Zhang, J.; Claverie, J.; Chaker, M.; Ma, D. Colloidal Metal Nanoparticles Prepared by Laser Ablation and their Applications. *ChemPhysChem* **2017**, *118*, 986-1006.
- (15) Nanoalloys: from fundamentals to emergent applications, 1<sup>st</sup> Ed., Calvo, F., Eds. Elsevier **2013**.
- (16) Xia, Y.; Xia, X.; Peng, H. C. Shape-Controlled Synthesis of Colloidal Metal Nanocrystals: Thermodynamic versus Kinetic Products. *J. Am. Chem. Soc.* **2015**, *137*, 7947-7966.
- (17) Choi, K. W.; Kang, S. W.; Kim, D. Y.; Im, S. H.; Park, Y.; Han, S. W.; Park, O. O. Size-controlled gold nano-tetradecapods with tunable optical and electromagnetic properties. *J. Mater. Chem. C* **2016**, *4*, 3149-3156.

(18) Abedini, A.; Bakar, A. A. A.; Larki, F.; Menon, P. S.; Islam, Md. S.; Shaari, S. Recent Advances in Shape-Controlled Synthesis of Noble Metal Nanoparticles by Radiolysis Route. *Nanoscale Res. Lett.* **2016**, *11*, 287-300.

(19) Clifford, D. C.; Castano, C. E.; Rojas, J. V. Supported transition metal nanomaterials: Nanocomposites synthesized by ionizing radiation. *Radiat. Phys. Chem.* **2017**, *132*, 52-64.

(20) Breitenkamp, M.; Henglein, A.; Lilie, J. Mechanism of the reduction of lead ions in aqueous solution (a pulse radiolysis study). *Ber. Bunsen. Phys. Chem.* **1976**, *80*, 973-979.

(21) Kelm, M.; Lilie, J.; Henglein, A.; Janata, E. Pulse radiolytic study of  $\text{Ni}^+$ . Nickel-carbon bond formation. *J. Phys. Chem-US* **1974**, *78*, 882-887.

(22) Belloni, J.; Mostafavi, M. Radiation Chemistry of Nanocolloids and Clusters, in Studies in Physical and Theoretical Chemistry 87. Radiation Chemistry: Present Status and Future Trends; Jonah, C. D. Rao, M. Eds.; Elsevier: New York, **2001** 411.

(23) Zhang, Z.; Nenoff, T. M.; Leung, K.; Ferreira, S.; Huang, J.; Berry, D. T.; Provencio, P.P.; Stumpf, R. Room-Temperature Synthesis of Ag–Ni and Pd–Ni Alloy Nanoparticles. *J. Phys. Chem. C* **2010**, *114*, 14309-14318.

(24) Jiao, D.; Leung, K.; Rempe, S. B.; Nenoff, T. M. First Principles Calculations of Atomic Nickel Redox Potentials and Dimerization Free Energies: A Study of Metal Nanoparticle Growth. *J. Chem. Theory Comput.* **2011**, *7*, 485-495.

(25) Leung, K.; Nenoff, T. M. Hydration structures of U(III) and U(IV) ions from ab initio molecular dynamics simulations. *J. Chem. Phys.* **2012**, *137*, 074502.

(26) Alivisatos, A. P. Semiconductor Clusters, Nanocrystals, and Quantum Dots. *Science* **1996**, *271*, 933-937.

(27) Henglein, A. Small-particle research: physicochemical properties of extremely small colloidal metal and semiconductor particles. *Chem. Rev.* **1989**, *89*, 1861-1873.

(28) Remita, H.; Lampre, I.; Mostafavi, M.; Balanzat, E.; Bouffard, S. Comparative study of metal clusters induced in aqueous solutions by  $\gamma$ -rays, electron or  $\text{C}_6^+$  ion beam irradiation. *Rad. Phys. Chem.* **2005**, *72*, 575-586.

(29) Misra, N.; Biswal, J.; Dhamgaye, V. P.; Lohda, G. S.; Sabharwal, S. A comparative study of gamma, electron beam, and synchrotron X-ray irradiation method for synthesis of silver nanoparticles in PVP. *Adv. Mater. Lett.* **2013**, *4*, 458-463.

(30) Gerasimov, Y. Radiation methods in nanotechnology. *J. Eng. Phys. Thermophys.* **2011**, *84*, 947-963.

(31) Abidi, W.; Remita, H. Gold based Nanoparticles Generated by Radiolytic and Photolytic Methods. *Recent Pat. Engin.* **2010**, *4*, 170-188.

(32) Belloni, J.; Mostafavi, M.; Remita, H.; Marignier, J. L.; Delcourt, M. O. Radiation-induced synthesis of mono- and multi-metallic clusters and nanocolloids. *New J. Chem.* **1998**, *22*, 1239-1255.

(33) Chen, Q.; Shen, X.; Gao, H. Radiolytic syntheses of nanoparticles in supramolecular assemblies. *Adv. Coll. Int. Sci.* **2010**, *159*, 32-44.

(34) Remita, H.; Remita, S. Chapter 13 : Metal clusters and nanomaterials: contribution of radiation chemistry in Recent trends in radiation chemistry; Whishart, J. F.; Rao, B. S. M. Eds. World Scientific Publishing Co. Pte. Ltd. **2010** 347-.

(35) Belloni, J. Metal nanocolloids. *Curr. Opin. Colloid Interface Sci.* **1996**, *1*, 184-196.

(36) Li, T.; Park, H. G.; Choi, S. H.  $\gamma$ -Irradiation-induced preparation of Ag and Au nanoparticles and their characterizations. *Mater. Chem. Phys.* **2007**, *105*, 325-330.

(37) Roy, K.; Lahiri, S. In situ gamma-radiation: one-step environmentally benign method to produce gold-palladium bimetallic nanoparticles. *Anal. Chem.* **2008**, *80*, 7504-7507.

(38) Treguer, M.; de Cointet, C.; Remita, H.; Khatouri, J.; Mostafavi, M.; Amblard, J.; Belloni, J. ; de Keyzer, J. R. Dose Rate Effects on Radiolytic Synthesis of Gold–Silver Bimetallic Clusters in Solution. *J. Phys. Chem. B* **1998**, *102*, 4310-4321.

(39) Ershov, B. G.; Abkhalimov, E. V. Nucleation of silver upon the reduction by hydrogen in aqueous polyphosphate-containing solutions: Formation of clusters and nanoparticles. *Colloid J.* **2007**, *69*, 579-584.

(40) Dey, G. R. Reduction of the copper ion to its metal and clusters in alcoholic media: A radiation chemical study. *Radiat. Phys. Chem.* **2005**, *74*, 172-184.

(41) De Waele, V.; Kecht, J.; Tahri, Z.; Mostafavi, M.; Bein, T.; Mintova, S. Diverse copper clusters confined in microporous nanocrystals. *Sensor. Actuat. B-Chem.* **2007**, *126*, 338-343.

(42) Seliverstov, A. F.; Sukhov, N. L.; Ershov, B. G. Aqueous Solutions of Colloidal Ruthenium: the Radiation–Chemical Preparation and Optical Absorption. *Colloid J.* **2002**, *64*, 781-783.

(43) Marignier, J. L.; Belloni, J.; Delcourt, M. O.; Chevalier, J. P. Microaggregates of non-noble metals and bimetallic alloys prepared by radiation-induced reduction. *Nature* **1985**, *317*, 344-345.

(44) Spinks, J. W. T.; Woods, R. J. Third ed.; University of Saskatchewan: Saskatoon, Saskatchewan, Canada, **1990**.

(45) Wishart, J. F. Tools for radiolysis studies. In *Radiation Chemistry: From Basics to Applications in Material and Life Sciences*, ed. Spotheim-Maurizot, M.; Mostafavi, M.; Belloni, J.; Douki, T. EDP Sciences **2008**, 17.

(46) Allen, A. O.; Van Nostrand, D. Company, Inc.: Princeton, New Jersey, **1961**.

(47) Nenoff, T. M.; Ferriera, S. R.; Huang, J.; Hanson, D. J. Formation of uranium based nanoparticles via gamma-irradiation. *J. Nucl. Mater.* **2013**, *442*, 162-167.

(48) Ma, Q.; Moldovan, N.; Mancini, D. C.; Rosenberg, R. A. Synchrotron-radiation-induced, selective-area deposition of gold on polyimide from solution. *Appl. Phys. Lett.* **2000**, *76*, 2014-2016.

(49) Wang, C. H.; Hua, T. E.; Chien, C. C.; Yu, Y. L.; Yang, T. Y.; Liu, C. J.; Leng, W. H.; Hwu, Y.; Yang, Y. C.; Kim, C. C.; et al. Aqueous gold nanosols stabilized by electrostatic protection generated by X-ray irradiation assisted radical reduction. *Mater. Chem. Phys.* **2007**, *106*, 323-329.

(50) Borse, P. H.; Yi, J. M.; Je, J. H.; Choi, S. D.; Hwu, Y.; Ruterana, P.; Nouet, G. Formation of magnetic Ni nanoparticles in x-ray irradiated electroless solution. *Nanotechnology* **2004**, *15*, 389-392.

(51) Karadas, F.; Ertas, G.; Ozkaraoglu, E.; Suzer, S. X-ray-induced production of gold nanoparticles on a SiO<sub>2</sub>/Si system and in a poly(methyl methacrylate) matrix. *Langmuir* **2005**, *21*, 437-442.

(52) Lee, H. J. ; Je, J. H.; Hwu, Y.; Tsai, W. L. Synchrotron X-ray induced solution precipitation of nanoparticles. *Nucl. Instrum. Meth. B* **2003**, *199*, 342-347.

(53) Wang, B. L.; Hsao, B. J.; Lai, S. F.; Chen, W. C.; Chen, .H H.; Chen, Y. Y.; Chien, C. C.; Cai, X.; Kampson, I. M.; Hwu, Y.; et al. One-pot synthesis of AuPt alloyed nanoparticles by intense x-ray irradiation. *Nanotechnology* **2011**, *22*, 065605.

(54) Zhang, J.; Dong, W.; Sheng, J.; Sheng, J.; Li, J.; Qiao, L.; Jiang, L. Silver nanoclusters formation in ion-exchanged glasses by thermal annealing, UV-laser and X-ray irradiation. *J. Cry. Grow.* **2008**, *310*, 234-239.

(55) Remita, S.; Fontaine, P.; Lacaze, E.; Borensztein, Y.; Sellame, H.; Farha, R.; Rochas, C.; Goldmann, M. X-ray radiolysis induced formation of silver nano-particles: A SAXS and UV visible absorption spectroscopy study. *Nucl. Instrum. Meth. B* **2007**, *263*, 436-440.

(56) Fong, Y. Y.; Visser, B. R.; Gascooke, J. R.; Cowie, B. C. C.; Thomsen, L.; Metha, G. F.; Buntine, M. A.; Harris, H. H. Photoreduction kinetics of sodium tetrachloroaurate under synchrotron soft X-ray exposure. *Langmuir* **2011**, *27*, 8099-8104.

(57) Ohkubo, Y.; Nakagawa, T.; Seino, S.; Kugai, J.; Yamamoto, T. A.; Nitani, H.; Niwa, Y. X-ray-induced reduction of Au ions in an aqueous solution in the presence of support materials and in situ time-resolved XANES measurements. *J. Synchrotron Radiat.* **2014**, *21*, 1148-1152.

(58) Ma, J.; Zou, Y.; Jiang, Z.; Huang, W.; Li, J.; Wu, G.; Huang, Y.; Xu, H. An in situ XAFS study--the formation mechanism of gold nanoparticles from X-ray-irradiated ionic liquid. *Phys. Chem. Chem. Phys.* **2013**, *15*, 11904-11908.

(59) Yamaguchi, A.; Matsumoto, T.; Okada, I.; Sakurai, I.; Utsumi, Y. Surface-enhanced Raman Scattering active metallic nanostructure fabricated by photochemical reaction of synchrotron radiation. *Mater. Chem. Phys.* **2015**, *160*, 205-211.

(60) Yamaguchi, A.; I. Okada, I.; T. Fukuoka; Sakurai, I.; Utsumi, Y. Synthesis of metallic nanoparticles through X-ray radiolysis using synchrotron radiation. *Jpn. J. appl. Phys.* **2016**, *55*, 055502.

(61) Tamai, T.; Watanabe, M.; Teramura, T.; Nishioka, N.; Matsukawa, K. Metal Nanoparticle/Polymer Hybrid Particles: The Catalytic Activity of Metal Nanoparticles Formed on the Surface of Polymer Particles by UV-Irradiation. *Macromol. Symp.* **2010**, *288*, 104-111.

(62) Abyaneh, M. K.; Paramanik, D.; Varma, S.; Gosavi, S. W.; Kulkarni, S. K. Formation of gold nanoparticles in polymethylmethacrylate by UV irradiation. *J. Phys. D Appl. Phys.* **2007**, *40*, 3771-3779.

(63) Ozkaraoglu, E.; Tunc, I.; Suzer, S. Preparation of Au and Au-Pt nanoparticles within PMMA matrix using UV and X-ray irradiation. *Polymer* **2009**, *50*, 462-466.

(64) Navaladian, S.; Viswanathan, B.; Varadarajan, T. K.; Viswanath, R. P. Fabrication of Worm-Like Nanorods and Ultrafine Nanospheres of Silver Via Solid-State Photochemical Decomposition. *Nanoscale Res. Lett.* **2009**, *4*, 471-479.

(65) Varma, R. S.; Kothari, D. C.; Choudhari, R. J.; Kumar, R.; Tewari, R.; Dey, G. K. Study of formation of Cu nanoparticle using Swift heavy ions. *Surf. Coat. Tech.* **2009**, *203*, 2468-2471.

(66) Dhara, S. Formation, Dynamics, and Characterization of Nanostructures by Ion Beam Irradiation. *Crit. Rev. Solid State* **2007**, *32*, 1-50.

(67) Dev, B. N.; Bera, S.; Satpati, B.; Goswami, D. K.; Bhattacharjee, K.; Satyam, P. V.; Yamashita, K.; Liedke, O. M.; Potzger, K.; Fassbender, J.; et al. Nonmagnetic to magnetic nanostructures via ion irradiation. *Microelectron. Eng.* **2006**, *83*, 1721-1725.

(68) Battaglin, G.; Cattaruzza, E.; Gonella, F.; Pollini, R.; D'Acapito, F.; Colonna, S.; Mattei, G.; Maurizio, C.; Mazzoldi, P.; Padovani, S.; et al. Silver nanocluster formation in ion-exchanged glasses by annealing, ion beam and laser beam irradiation: An EXAFS study. *Nucl. Instrum. Meth. B* **2003**, *200*, 185-190.

(69) Hanh, T. T.; Thu, N. T.; Quoc, L. A.; Hien, N. Q. Synthesis and characterization of silver/diatomite nanocomposite by electron beam irradiation. *Rad. Phys. Chem.* **2017**, *139*, 141-146.

(70) Lee, S. B.; Park, J.; van Aken, P. A. Formation of Pt–Zn Alloy Nanoparticles by Electron-Beam Irradiation of Wurtzite ZnO in the TEM. *Nano. Res. Lett.* **2016**, *11*, 339.

(71) Maguire, P.; Rutherford, D.; Macias-Montero, M.; Mahony, C.; Kelsey, C.; Tweedie, M.; Mariotti, D. Continuous In-Flight Synthesis for On-Demand Delivery of Ligand-Free Colloidal Gold Nanoparticles. *Nano Lett.* **2017**, *17*, 1336-1343.

(72) Mirdamadi-Esfahani, M.; Mostafavi, M.; Keita, B.; Nadjo, L.; Kooyman, P.; Remita, H. Bimetallic Au-Pt nanoparticles synthesized by radiolysis: Application in electro-catalysis. *Gold Bull.* **2010**, *43*, 49-56.

(73) Kageyama, S.; Seino, S.; Nakagawa, T.; Nitani, H.; Ueno, K.; Daimon, H.; Yamamoto, T. A. Formation of PtRu alloy nanoparticle catalyst by radiolytic process assisted by addition of dl-tartaric acid and its enhanced methanol oxidation activity. *J. Nanopart. Res.* **2011**, *13*, 5275-5287.

(74) Kugai, J.; Kubota, C.; Okazaki, T.; Seino, S.; Nakagawa, T.; Nitani, H.; Yamamoto, T. A. Effect of reduction enhancer on a radiolytic synthesis of carbon-supported Pt–Cu nanoparticles and their structural and electrochemical properties. *J. Nanopart. Res.* **2015**, *17*, 239.

(75) Kugai, J.; Dodo, E.; Seino, S.; Nakagawa, T.; Okazaki, T.; Yamamoto, T. A. Effect of organic stabilizers on Pt–Cu nanoparticle structure in liquid-phase syntheses: control of crystal growth and copper reoxidation. *J. Nanopart. Res.* **2016**, *18*, 62.

(76) Ershov, B. G.; Janata, E.; Henglein, A.; Fojtik, A. Silver atoms and clusters in aqueous solution: absorption spectra and the particle growth in the absence of stabilizing  $\text{Ag}^+$  ions. *J. Phys. Chem.* **1993**, *97*, 4589-4594.

(77) Gachard, E.; Remita, H.; Khatouri, J.; Keita, B.; Nadjo, L.; Belloni, J. Radiation-induced and chemical formation of gold clusters. *New J. Chem.* **1998**, *22*, 1257-1265.

(78) Jellinek, J. Nanoalloys: tuning properties and characteristics through size and composition. *Faraday Discuss.* **2008**, *138*, 11-35.

(79) Remita, H.; Etcheberry, A.; Belloni, J. Dose Rate Effect on Bimetallic Gold–Palladium Cluster Structure. *J. Phys. Chem. B* **2003**, *107*, 31-36.

(80) Redjala, T.; Remita, H.; Apostolescu, G.; Mostafavi, M.; Thomazeau, C.; Uzio, D. Bimetallic Au-Pd and Ag-Pd Clusters Synthesised by or Electron Beam Radiolysis and Study of the Reactivity/Structure Relationships in the Selective Hydrogenation of Buta-1,3-Diene. *Oil Gas Sci. Technol.* **2006**, *61*, 789-797.

(81) Ksar, F.; Ramos, L.; Keita, B.; Nadjo, L.; Beaunier, P.; Remita, H. Bimetallic Palladium-Gold Nanostructures: Application in Ethanol Oxidation. *Chem. Mater.* **2009**, *21*, 3677-3683.

(82) Zhang, Z. Y.; Nenoff, T. M.; Huang, J. Y.; Berry, D. T.; Provencio, P. P. Room Temperature Synthesis of Thermally Immiscible Ag–Ni Nanoalloys. *J. Phys. Chem. C* **2009**, *113*, 1155-1159.

(83) Sims, C. T.; Stoloff, N. S.; Hagel, W. C. John Wiley & Sons **1987**.

(84) Chen, Y.; Palmer, R. E.; Wilcoxon, J. P. Sintering of passivated gold nanoparticles under the electron beam. *Langmuir* **2006**, *22*, 2851-2855.

(85) Jung, S.; Kim, J. H. Sintering characteristics of TiO<sub>2</sub> nanoparticles by microwave processing. *Korean J. Chem. Eng.* **2010**, *27*, 645-650.

(86) Coutts, M. J.; Cortie, M. B.; Ford, M. J.; McDonagh, A. M. Rapid and Controllable Sintering of Gold Nanoparticle Inks at Room Temperature Using a Chemical Agent. *J. Phys. Chem. C* **2009**, *113*, 1325-1328.

(87) Wakuda, D.; Hatamura, M.; Suganuma, K. Novel method for room temperature sintering of Ag nanoparticle paste in air. *Chem. Phys. Lett.* **2007**, *441*, 305-308.

(88) Fang, Z. Z.; Wang, H. Densification and grain growth during sintering of nanosized particles. *Int. Mater. Rev.* **2008**, *53*, 326-352.

(89) Ida, K.; Sugiyama, Y.; Chujyo, Y.; Tomonari, M.; Tokunaga, T.; Sasaki, K.; Kuroda, K. In-situ TEM studies of the sintering behavior of copper nanoparticles covered by biopolymer nanoskin. *J. Electron. Microsc.* **2010**, *59*, S75-S80.

(90) Yeadon, M.; Yang, J. C.; Averback, R. S.; Gibson, J. M. Techniques for Studying Nanoparticle Sintering by Plan-View In Situ Transmission Electron Microscopy. *Microsc. Microanal.* **1998**, *4*, 248-253.

(91) Nenoff, T. M.; Zhang, Z.; Leung, K.; Stumpf, R.; Huang, J.; Lu, P.; Berry, D. T.; Provencio, P. P.; Hanson, D.; Robinson, D.; et al. Room Temperature Synthesis of Ni-based Alloy Nanoparticles by Radiolysis; Sandia National Laboratories: SAND2009-6424, Albuquerque **2009**

(92) Nenoff, T. M.; Jacobs, B. W.; Robinson, D. B.; Provencio, P. P.; Huang, J.; Ferreira, S.; Hanson, D. J. Synthesis and Low Temperature In Situ Sintering of Uranium Oxide Nanoparticles. *Chem. Mater.* **2011**, *23*, 5185-5190.

(93) Michalik, J.; Sadlo, J.; Danilczuk, M.; Perlinska, J.; Yamada, H. Cationic silver clusters in zeolite RHO and sodalite. *Stud. Surf. Sci. Catal. A* **2002**, *142*, 311-318.

(94) Vijayalakshmi, R.; Kapoor, S.; Kulshreshtha, S. K. Radiolytic preparation of nanosized Pt particles in sodium zeolite A. *Solid State Sci.* **2002**, *4*, 489-494.

(95) Hornebecq, V.; Antonietti, M.; Cardinal, T.; Treguer-Delapierre, M. Stable silver nanoparticles immobilized in mesoporous silica. *Chem. Mater.* **2003**, *15*, 1993-1999.

(96) Benoit, R.; Warmont, F.; Meynen, V.; De Witte, K.; Cool, P. Treguer-Delapierre, M.; Saboungi, M. Optimisation of the surface properties of SBA-15 mesoporous silica for in-situ nanoparticle synthesis. *Microp. Mesop. Mater.* **2009**, *120*, 2-6.

(97) Abidi, W.; Pansu, B.; Krishnaswamy, R.; Beaunier, P.; Remita, H.; Impérator-Clerc, M. Gold nanoparticles confined in lamellar mesophases. *RSC Adv.* **2011**, *1*, 434-439.

(98) Attia, J.; Remita, S.; Jonic, S.; Lacaze, E.; Fauré, M.; Larquet, E.; Goldmann, M. Radiation-induced synthesis and Cryo-TEM characterization of silver nanoshells on linoleate spherical micelles. *Langmuir* **2007**, *23*, 9523-9526.

(99) Platzer, O.; Amblard, J.; Marignier, J. L.; Belloni, J. Nanosecond pulse radiolysis study of metal aggregation in polymeric membranes. *J. Phys. Chem.* **1992**, *96*, 2334-2340.

(100) Hund, J. F.; Bertino, M. F.; Zhang, G.; Sotiriou-Leventis, C.; Leventis, N.; Tokuhiro, A. T.; Farmer, J. Formation and entrapment of noble metal clusters in silica aerogel monoliths by  $\gamma$ -radiolysis. *J. Phys. Chem. B* **2003**, *107*, 465-469.

(101) Oh, S. D.; Yoon, K. R.; Choi, S. H.; Gopalan, A.; Lee, K. P.; Sohn, S. H.; Kang, H. D.; Choi, I. S. Dispersion of Pt-Ru alloys onto various carbons using  $\gamma$ -irradiation. *J. Non-Cryst. Solids* **2006**, *352*, 355-360.

(102) Seo, K. D.; Oh, S. D.; Choi, S. H.; Kim, S. H.; Park, H. G.; Zhang, Y. P. Radiolytic loading of the Pt-Ru nanoparticles onto the porous carbons. *Colloids Surf. A* **2008**, *313-315*, 393-397.

(103) Bae, H. B.; Ryu, J. H.; Byun, B. S.; Choi, S. H.; Kim, S. H.; Hwang, C. G. Radiolytic Deposition of Pt-Ru Catalysts on the Conductive Polymer Coated MWNT and their Catalytic Efficiency for CO and MeOH. *Adv. Mater. Res.* **2008**, *47-50*, 1478-1481.

(104) Yang, D. S.; Sim, K. S.; Kw En, H. D.; Choi, S. H. One-step preparation of Pt–M@FP-MWNT catalysts (M=Ru, Ni, Co, Sn, and Au) by  $\gamma$ -ray irradiation and their catalytic efficiency for CO and MeOH. *J. Ind. Eng. Chem.* **2012**, *18*, 538-545.

(105) Ghosh, S.; Natalie, K. A.; Ramos, L.; Remita, S.; Dazzi, A.; Besseau, A. D.; Goubard, F.; Aubert, P. H.; Remita, H. Conducting polymer nanostructures for photocatalysis under visible light. *Nat. Mater.* **2015**, *14*, 505-511.

(106) Ghosh, S.; Thandavarayan, M.; Basu, R. N. Nanostructured conducting polymers for energy applications: towards a sustainable platform. *Nanoscale* **2016**, *8*, 6921-6947.

(107) Hable, C. T.; Wrighton, M. S. Electrocatalytic oxidation of methanol and ethanol: a comparison of platinum-tin and platinum-ruthenium catalyst particles in a conducting polyaniline matrix. *Langmuir* **1993**, *3*, 3284-3290.

(108) Xu, H.; Wang, A. L.; Tong, Y. X.; Li, G. R. Enhanced Catalytic Activity and Stability of Pt/CeO<sub>2</sub>/PANI Hybrid Hollow Nanorod Arrays for Methanol Electro-oxidation. *ACS Catal.* **2016**, *6*, 5198-5206.

(109) Oh, S. D.; So, B. K.; Choi, S. H.; Gopalan, A.; Lee, K. P.; Ro Yoon, K.; Choi, I. S. Dispersing of Ag, Pd, and Pt-Ru alloy nanoparticles on single-walled carbon nanotubes by  $\gamma$ -irradiation. *Mater. Lett.* **2005**, *59*, 1121-1124.

(110) Seino, S.; Imoto, Y.; Kitagawa, D.; Kubo, Y.; Kosaka, T.; Kojima, T.; Yamamoto, T. A. Radiochemical synthesis of silver nanoparticles onto textile fabrics and their antibacterial activity. *J. Nucl. Sci. Technol.* **2016**, *53*, 1021-1027.

(111) Grabowska, E.; Zaleska, A.; Sorgues, S.; Kunst, M.; Etcheberry, A.; Colbeau-Justin, C.; Remita, H. Modification of Titanium(IV) Dioxide with Small Silver Nanoparticles: Application in Photocatalysis. *J. Phys. Chem. C* **2013**, *117*, 1955-1962.

(112) Hai, Z.; El Kolli, N.; Chen, J.; Remita, H. Radiolytic synthesis of Au–Cu bimetallic nanoparticles supported on TiO<sub>2</sub>: application in photocatalysis. *New J. Chem.* **2014**, *38*, 5279-5286.

(113) Luna, A. L.; Novoseltceva, E.; Louarn, E.; Beaunier, P.; Kowalska, E.; Ohtani, B.; Colbeau-Justin, C. Synergetic Effect of Ni and Au Nanoparticles Synthesized on Titania Particles for Efficient Photocatalytic Hydrogen Production. *Appl. Catal. B: Environ.* **2016**, *191*, 18-28.

(114) Rao, V. M.; Castano, C. H.; Rojas, J.; Abdulghani, A. Synthesis of nickel nanoparticles on multi-walled carbon nanotubes by gamma irradiation. *J. Rad. Phys. Chem.* **2013**, *89*, 51-56.

(115) Yamamoto, T. A.; Seino, T. S.; Nitani, H. Bimetallic Nanoparticles Of PtM (M = Au, Cu, Ni) Supported on Iron Oxide: Radiolytic Synthesis and CO Oxidation Catalysis. *Appl. Catal. A: Gen.* **2010**, *387*, 195-202.

(116) Ghosh, S.; Bera, S.; Bysakh, S.; Basu, R. N. Highly active multimetallic palladium nanoalloys embedded in conducting polymer as anode catalyst for electrooxidation of ethanol. *ACS Appl. Mater. Interf.* **2017**, *9*, 33775-33790.

(117) Ghosh, S.; Bera, S.; Bysakh, S.; Basu, R. N. Conducting polymer nanofiber-supported Pt alloys: unprecedented materials for methanol oxidation with enhanced electrocatalytic performance and stability. *Sustainable Energy Fuels* **2017**, *1*, 1148-1161.

(118) Lehoux, A.; Ramos, L.; Beaunier, P.; Uribe, D. B.; Dieudonné, P.; Audonnet, F.; Etcheberry, A.; José-Yacaman, M.; Remita, H. Tuning the porosity of bimetallic nanostructures by a soft templating approach. *Adv. Funct. Mater.* **2012**, *22*, 4900-4908.

(119) Chen, L. Y.; Xu, Z. X.; Dai, H.; Zhang, S. T. Facile synthesis and magnetic properties of monodisperse  $\text{Fe}_3\text{O}_4$ /silica nanocomposite microspheres with embedded structures via a direct solution-based route. *J. Alloys Compd.* **2010**, *497*, 221-227.

(120) Benguedouar, Y.; Keghouche, N.; Belloni, J. Structural and magnetic properties of Ni–Pt nanoalloys supported on silica. *Mater. Sci. Eng. B* **2012**, *177*, 27-33.

(121) Lee, K. P.; Lee, S. H.; Sundaram, K. S.; Gopalan, A.; Iyengar, A. Preparation of Co/Pd alloy particles dispersed multiwalled carbon nanotube supported nanocatalysts via gamma irradiation. *Rad. Phys. Chem.* **2012**, *81*, 1422-1425.

(122) Ghosh, S.; Holade, Y.; Remita, H.; Servat, K.; Beaunier, P.; Hagège, A.; Kokoh, K. B.; Napporn, T. W. One-pot synthesis of reduced graphene oxide supported gold-based nanomaterials as robust nanocatalysts for glucose electrooxidation. *Electrochimica Acta* **2016**, *212*, 864-875.

(123) Rotureau, P.; Renault, J. P.; Lebeau, B.; Patarin, J.; Mialocq, J. Radiolysis of confined water: molecular hydrogen formation. *ChemPhysChem* **2005**, *6*, 1316-1323.

(124) Thomas, J. K. Physical Aspects of Radiation-Induced Processes on  $\text{SiO}_2$ ,  $\gamma\text{-Al}_2\text{O}_3$ , Zeolites, and Clays. *Chem. Rev.* **2005**, *105*, 1683-1734.

(125) Tahri, Z.; Luchez, F.; Yordanov, I.; Poizat, O.; Moissette, A.; Valtchev, V.; De Waele, V. Nanosecond probing of the early nucleation steps of silver atoms in colloidal zeolite by pulse radiolysis and flash photolysis techniques. *Res. Chem. Intermed.* **2009**, *35*, 379-388.

(126) Kecht, J.; Tahri, Z.; De Waele, V.; Mostafavi, M.; Mintova, S.; Bein, T. Colloidal Zeolites as Host Matrix for Copper Nanoclusters. *Chem. Mater.* **2006**, *18*, 3373-3380.

(127) Yordanov, I.; Knoerr, R.; De Waele, V.; Bazin, P.; Thomas, S.; Rivallan, M.; Mintova, S. Elucidation of Pt Clusters in the Micropores of Zeolite Nanoparticles Assembled in Thin Films. *J. Phys. Chem. C* **2010**, *114*, 20974-20982.

(128) Knoerr, R.; Yordanov, I.; De Waele, V.; Mintova, S.; Mostafavi, M. Preparation of Colloidal BEA Zeolite Functionalized with Pd Aggregates as a Precursor for Low Dimensionality Sensing Layer. *Sens. Lett.* **2010**, *8*, 497-501.

(129) Li, S.; Tuel, A.; Rousset, J. L.; Morfin, F.; Aouine, M.; Burel, L.; Meunier, F.; Farrusseng, D. Hollow Zeolite Single-Crystals Encapsulated Alloy Nanoparticles with Controlled Size and Composition. *ChemNanoMat* **2016**, *2*, 534-539.

(130) Dey, G. R.; El Omar, A. K.; Jacob, J. A.; Mostafavi, M.; Belloni, J. Mechanism of trivalent gold reduction and reactivity of transient divalent and monovalent gold ions studied by gamma and pulse radiolysis. *J. Phys. Chem. A* **2011**, *115*, 383-391.

(131) Bresin, M.; Chamberlain, A.; Donev, E. U.; Samantaray, C. B.; Schariden, G. S.; Hastings, J. T. Electron-Beam-Induced Deposition of Bimetallic Nanostructures from Bulk Liquids. *Angew. Chem. Inter. Ed.* **2013**, *52*, 8004-8007.

(132) Henglein, A.; Meisel, D. Radiolytic Control of the Size of Colloidal Gold Nanoparticles. *Langmuir* **1998**, *14*, 7392-7396.

(133) Butler, J.; Henglein, A. Elementary reactions of the reduction of  $\text{Tl}^+$  in aqueous solution. *Radiat. Phys. Chem.* **1980**, *15*, 603-612.

(134) Hart, E. The Hydrated Electron: Properties and reactions of this most reactive and elementary of aqueous negative ions are discussed. *Science* **1964**, *146*, 19-25.

(135) Schwarz, H. A.; Dodson, R. W. Reduction potentials of CO<sub>2</sub>- and the alcohol radicals. *J. Phys. Chem.* **1989**, *93*, 409-414.

(136) Turkevich, J.; Stevenson, P. C.; Hillier, J. A study of the nucleation and growth processes in the synthesis of colloidal gold. *Discuss. Faraday Soc.* **1951**, *11*, 55-75.

(137) Turkevich, J. Colloidal gold. Part I. *Gold Bull.* **1985**, *18*, 86-91.

(138) Henglein, A. Reactions of organic free radicals at colloidal silver in aqueous solution. Electron pool effect and water decomposition. *J. Phys. Chem.* **1979**, *83*, 2209-2216.

(139) Henglein, A. Colloidal Palladium Nanoparticles: Reduction of Pd(II) by H<sub>2</sub>; Pd<sub>Core</sub>Au<sub>Shell</sub>Ag<sub>Shell</sub> Particles. *J. Phys. Chem. B* **2000**, *104*, 6683-6685.

(140) Remita, H.; Etcheberry, A.; Belloni, J. Dose Rate Effect on Bimetallic Gold–Palladium Cluster Structure. *J. Phys. Chem. B* **2003**, *107*, 31-36.

(141) Hansen, M.; Anderko, K. Second Edition ed.; McGraw-Hill Book Company: New York, **1958**.

(142) Henglein, A. Electron transfer in heterogeneous photochemical reactions. *Ber. Bunsen. Phys. Chem.* **1977**, *81*, 556-561.

(143) Spasov, V.; Lee, T.; Maberry, J.; Ervin, K. Measurement of the dissociation energies of anionic silver clusters (Ag<sub>n</sub><sup>-</sup>, n=2–11) by collision-induced dissociation. *J. Chem. Phys.* **1999**, *110*, 5208.

(144) Larsen, J.; Ranney, J.; Starr, D.; Musgrove, J.; Campbell, C. Adsorption energetics for Ag on MgO(100). *Phys. Rev. B* **2001**, *63*, 195410-195417.

(145) Ershov, B. G. Aqueous solutions of colloidal nickel: radiation-chemical preparation, absorption spectra, and properties. *Russ. Chem. B.* **2000**, *49*, 1715-1721.

(146) Henglein, A.; Giersig, M. Formation of Colloidal Silver Nanoparticles: Capping Action of Citrate. *J. Phys. Chem. B* **1999**, *103*, 9533.

(147) Burda, C.; Chen, X.; Narayanan, R.; El-Sayed, M. A. Chemistry and Properties of Nanocrystals of Different Shapes. *Chem. Rev.* **2005**, *105*, 1025-1102.

(148) Liu, Y.; Li, D.; Sun, S. Pt-based composite nanoparticles for magnetic, catalytic, and biomedical Applications. *J. Mater. Chem.* **2011**, *21*, 12579-12587.

(149) Zhong, C. J.; Luo, J.; Fang, B.; Wanjala, B. N.; Njoki, P. N.; Loukrakpam, R.; Yin, J. Nanostructured catalysts in fuel cells. *Nanotechnology* **2010**, *21*, 062001.

(150) Le Gratiet, B.; Remita, H.; Picq, G.; Delcourt, M. O. Pt and Pt/Cu carbonyl clusters synthesized by radiolysis. *Radiat. Phys. Chem.* **1996**, *47*, 263-268.

(151) Merga, G.; Milosavljevic, B. H.; Meisel, D. Radiolytic hydrogen yields in aqueous suspensions of gold particles. *J. Phys. Chem. B* **2006**, *110*, 5403-5408.

(152) Merga, G.; Wilson, R.; Lynn, G.; Milosavljevic, B. H.; Meisel, D. Redox Catalysis on “Naked” Silver Nanoparticles. *J. Phys. Chem. C* **2007**, *111*, 12220-12226.

(153) Kapoor, S.; Barnabas, F. A.; Sauer, M. C.; Meisel, D.; Jonah, C. D. Kinetics of Hydrogen Formation from Formaldehyde in Basic Aqueous Solutions; *J. Phys. Chem.* **1995**, *99*, 6857-6883.

(154) Sinha, A. K.; Suzuki, K.; Takahara, M.; Azuma, H.; Nonaka, T.; Fukumoto, K. Mesostructured manganese oxide/gold nanoparticle composites for extensive air purification. *Angew. Chem.* **2007**, *119*, 2949-2952.

(155) Kamat, P. V.; Meisel, D. Nanoscience opportunities in environmental remediation. *CR Chim.* **2003**, *6*, 999-1007.

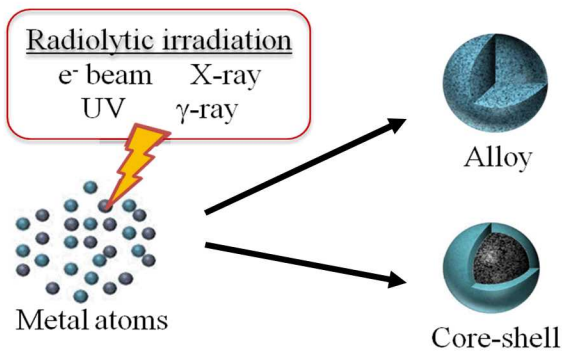
(156) Liu, M.; Zhang, R.; Chen, W. Graphene-Supported Nanoelectrocatalysts for Fuel Cells: Synthesis, Properties, and Applications. *Chem. Rev.* **2014**, *114*, 5117-5160.

(157) Zhang, J.; Worley, J.; Denommee, S.; Kingston, C.; Jakubek, Z. J.; Deslandes, Y.; Post, M.; Simard, B.; Braidy, N.; Botton, G. A. Synthesis of Metal Alloy Nanoparticles in Solution by Laser Irradiation of a Metal Powder Suspension. *J. Phys. Chem. B* **2003**, *107*, 6920-6923.

(158) Remita, S.; Picq, G.; Khatouri, J.; Mostafavi, M. Radiolytic formation of bilayered  $\text{Pt}_{\text{core}}/\text{Au}_{\text{shell}}$  and  $\text{Au}_{\text{core}}/\text{Pt}_{\text{shell}}$  clusters in aqueous solution. *Rad. Phys. Chem.* **1999**, *54*, 463-473.

(159) Chettibi, S.; Wojcieszak, R.; Boudjennad, E. H.; Belloni, J.; Bettahar, M. M.; Keghouche, N. Catalytic properties of  $\text{CeO}_2$ - supported nickel clusters synthesized by radiolysis. *Catal. Today* **2006**, *113*, 157-165.

## Table of Contents (TOC) Graphic



## Biographies



Julien Grand received his Ph.D. degree in organic chemistry from Laboratoire de Chimie Moléculaire et Thioorganique (LCMT) of Caen (France) in 2013 and is currently working as a research engineer in Laboratoire de Catalyse et Spectrochimie (LCS) of Caen (France). His main research interests are porous materials synthesis and their applications as sensing materials.



Summer Ferreira received her Ph.D. in Materials Science and Engineering from the University of Illinois Urbana-Champaign in 2009. She is a Principal Staff Member at Sandia National Laboratories where her primary focus is in studying the risks of electrochemical energy storage devices.



Vincent De Waele received a PhD degree in 1999 from the University of Lille, in the field of photochemistry and ultrafast spectroscopy under the supervision of Dr O. Poizat. From 2000 to 2002 he worked as Humboldt and Marie Curie fellows in the group of Pr. E. Riedle where he applied ultrafast transient absorption spectroscopy to the investigation of the photoreactivity in nanozeolites. In 2002, he joined the group of M. Mostafavi and developed ultrafast pulse radiolysis experiments notably to study of the radiolytic growth of metal NPs in porous materials. Since 2009, V. De Waele is CNRS researcher at Laboratory of Spectroscopy Infrared and Raman (LASIR). His current scientific interests concern the photoactive host-guest materials, and in particular the zeolites functionalized with metal or semi-conductor nanoparticles.



Svetlana Mintova is Director of Research 1<sup>st</sup> class in CNRS, Laboratory of Catalysis and Spectroscopy, Normandy University, ENSICAEN, Caen, France and Thousand Talent Professor in China University of Petroleum, College of Chemical Engineering, Qingdao, China. Receiver of the Donald Breck award from the International Zeolite Association (IZA, 2016), Baron Cronstedt award from the Federation of European Zeolite Associations (FEZA, 2014). Her scientific interests include preparation of nanosized zeolites, films, coatings, composites and related advanced applications.



Tina M. Nenoff is a Senior Scientist in the Materials, Chemicals and Physics Center at Sandia National Laboratories in Albuquerque, NM, USA. She is a Fellow of the American Chemical Society (2011), an Associate Editor of *Industrial and Chemical Engineering Research* (ACS journal), and was profiled in “Successful Women Ceramic and Glass Scientists and Engineers: 100 Inspirational Profiles” (Wiley, 2016). Her scientific interests include the synthesis and characterization of nanoscale materials (nanoporous and nanoparticles), the chemistry that occurs at the nanoscale, and how that chemistry relates to bulk scale performance in both energy and environmental applications.